IEEE Access
Multidisciplinary | Rapid Review | Open Access Journal

Received December 4, 2019, accepted December 10, 2019, date of publication January 6, 2020, date of current version January 21, 2020.

Digital Object Identifier 10.1109/ACCESS.2020.2964149

Experimental and Analytical Investigations of an Optically Pre-Amplified FSO-MIMO System With Repetition Coding Over Non-Identically Distributed Correlated Channels

RICHA PRIYADARSHANI[1], (Student Member, IEEE), MANAV R. BHATNAGAR[1], (Senior Member, IEEE), JAN BOHATA[2], (Member, IEEE), STANISLAV ZVANOVEC[2], (Senior Member, IEEE), AND ZABIH GHASSEMLOOY[3], (Senior Member, IEEE)

[1]Department of Electrical Engineering, Indian Institute of Technology Delhi, New Delhi 110016, India
[2]Department of Electromagnetic Field, Faculty of Electrical Engineering, Czech Technical University in Prague, 16627 Prague, Czech Republic
[3]Optical Communications Research Group, Faculty of Engineering and Environment, Northumbria University, Newcastle upon Tyne NE1 8ST, U.K.

Corresponding author: Richa Priyadarshani (richa.priyadarshani@ee.iitd.ac.in)

This work was supported in part by the Media Lab Asia (Sir Visvesvaraya Young Faculty Research Fellowship) through the Ministry of Electronics and Information Technology (MeiTY), Government of India, and in part by the Brigadier Bhopinder Singh Chair Professor.

ABSTRACT This paper presents theoretical and experimental bit error rate (BER) results for a free-space optical (FSO) multiple-input-multiple-output system over an arbitrarily correlated turbulence channel. We employ an erbium-doped fiber amplifier at the receiver (Rx), which results in an improved Rx's sensitivity at the cost of an additional non-Gaussian amplified spontaneous emission noise. Repetition coding is used to combat turbulence and to improve the BER performance of the FSO links. A mathematical framework is provided for the considered FSO system over a correlated non-identically distributed Gamma-Gamma channel; and analytical BER results are derived with and without the pre-amplifier for a comparative study. Moreover, novel closed-form expressions for the asymptotic BER are derived; a comprehensive discussion about the diversity order and coding gain is presented by performing asymptotic analysis at high signal-to-noise ratio (SNR). To verify the analytical results, an experimental set-up of a 2×1 FSO-multiple-input-single-output (MISO) system with pre-amplifier at the Rx is developed. It is shown analytically that, both correlation and pre-amplification do not affect the diversity order of the system, however, both factors have contrasting behaviour with respect to coding gain. Further, to achieve the target forward error correction BER limit of 3.8×10^{-3}, a 2×1 FSO-MISO system with a pre-amplifier requires 6.5 dB lower SNR compared with the system with no pre-amplifier. Moreover, an SNR penalty of 2.5 dB is incurred at a higher correlation level for the developed 2×1 experimental FSO set-up, which is in agreement with the analytical findings.

INDEX TERMS Arbitrary correlation, ASE noise, diversity, experimental, free-space optical communications, gamma-gamma distribution, optical pre-amplifier, spatial diversity.

I. INTRODUCTION

Regardless of all the advantages that a free-space optical (FSO) communications system offers such as high data rates, security at the physical layer, and license free spectrum; the quality of transmission of FSO link is exacerbated by the unpredictable weather conditions such as haze, fog, turbulence, thus resulting in system performance degradation because of signal fading and dispersion [1]–[3]. In order to characterize channel induced fading in FSO links, several statistical turbulence models have been proposed in the literature. Gamma-Gamma ($\Gamma\Gamma$) turbulence model has been proved as the most appropriate, which covers weak-to-strong turbulence regimes [1], [4]. Many spatial diversity techniques

The associate editor coordinating the review of this manuscript and approving it for publication was Huaqing Li.

are available in the literature, which employ multiple apertures at the transmitter (Tx) and/or at the receiver (Rx). These techniques are used to alleviate the effects of atmospheric turbulence (AT) and thereby improve the performance of FSO system [5]–[7]. A space-only code has been used to achieve a full spatial diversity gain in an intensity modulation/direct detection (IM/DD) multiple-input multiple-output (MIMO) system [8]. The full spatial diversity is achieved by using repetition codes (RC), where the same symbol is transmitted by all Tx apertures [9] – thus resulting in a fast maximum-likelihood (ML) detection. In [10] and [11], it has been reported that the RC outperforms the orthogonal space-time block code (OSTBC) in IM/DD FSO systems with on-off keying (OOK) and subcarrier intensity modulated multiple-input-single-output (MISO) systems.

There are many practical applications with multiple apertures, where the available space at the Tx/Rx end is not sufficient to employ apertures with proper separation between them (i.e., spatial coherence separation between them exceeding the fading correlation length) [1], [12]. Therefore, this limitation can lead to correlated FSO links. Hence, in order to ensure that the analysis carried out is generalized and also valid for a practical FSO system, channels must be considered to be correlated. In [4], the outage performance analysis of a selection combining-based Rx over a constant correlated $\Gamma\Gamma$ AT link was carried out. The performance analysis of diversity systems over a $\Gamma\Gamma$ AT channel was studied in [13] and [14]. The authors in [13] considered an exponentially correlated fading channel model to investigate the outage probability and the bit error rate (BER) of the selection combining and maximal ratio combining-based Rxs, respectively. While in [14] $\Gamma\Gamma$ random variables (RVs) were considered to be independent; performance analysis of sum of correlated $\Gamma\Gamma$ RVs was studied in [15] by using an approximate α-μ distribution for a triple aperture system. Performance analysis of multivariate $\Gamma\Gamma$ RVs with arbitrary correlation was presented in [16]. Although in [17], the BER analysis of the FSO-MISO system with RC was carried out over correlated $\Gamma\Gamma$ turbulence, the analysis was applicable only for constant correlation. The effect of the pointing error on the performance of FSO systems using multi-pulse pulse position modulation (MP-PPM) over the $\Gamma\Gamma$ turbulence channel was studied in [18]. The authors in [19] proposed an adaptive transmission modulation (ATM) technique for FSO links in order to improve the spectral efficiency of the system.

The use of an optical pre-amplifier at the Rx compensates for the losses incurred by the propagating wave; therefore, maintains the required receiver sensitivity and improves the data rate or the transmission span. However, it introduces an additional amplified spontaneous emission (ASE) noise, which results in the beat noises (i.e., spontaneous-spontaneous and signal-spontaneous) at the Rx. The received signal at the output of photo-detector is more precisely described by Chi-square distribution, when beat noises are dominant at the Rx (i.e., the dominant source compared to the shot and thermal noises) [20]–[22]. Non-Gaussian nature of the probability density functions (pdfs) of signals (i.e., logical 1's and 0's) in the presence of ASE noise has been experimentally verified in [23]. The BER of the indoor lightwave communications system employing optical pre-amplifiers and no turbulence was evaluated in [20], [21]. The effect of turbulence was considered in [22] in carrying out the BER analysis for a FSO system with ASE noise. The authors in [24]–[27] studied the effect of turbulence and pointing error on the BER performance of an optically pre-amplified FSO system by considering different distributions to model the FSO channel. However, all these analyses were based on a single-input-single-output (SISO) link and applicable to an un-correlated channel.

In this paper, we consider OOK IM/DD non-identical FSO links over the arbitrarily correlated $\Gamma\Gamma$ AT channel in the presence of ASE noise. Note that, in order to study a practical system, we have assumed that the number of line-of-sight photons (non-dispersed) is sufficiently higher than the number of the scattered photons at the Rx and the transmit power is sufficient to reduce the effect of dispersion [28], [29]. Therefore, both the AT and spatial correlation are considered as the dominant factors affecting the performance of the proposed FSO system. To the best of the authors' knowledge, the comparative BER performance analysis of a correlated FSO-MIMO system with RC and non-identical links, with and without the ASE noise has not been reported in the literature yet. It should be noted that, the considered correlated system model in this work is practically applicable to the terrestrial FSO links.

Motivated by aforesaid discussions, we claim the following specific contributions in this paper:

- Under the influence of arbitrary correlation, a novel closed-form analytical expression is derived for the BER of FSO-MIMO system with RC over the arbitrarily correlated $\Gamma\Gamma$ channel, without considering a pre-amplifier at the Rx.
- In order to generalize the analysis for the practical applications, the BER expression for the correlated FSO-MIMO system with a pre-amplifier is also derived in the form of power series.
- To substantiate the analytical findings, an experimental set-up is developed to validate the BER of a 2×1 correlated FSO system with RC in the presence of pre-amplifier at the Rx.
- Asymptotic BER analysis at high signal-to-noise ratio (SNR) is also performed to obtain expressions for the diversity gain, coding gain and the loss in coding gain. Useful insights into the impact of correlation and the ASE noise on the diversity and coding gains of the FSO-MIMO system are extracted with the help of asymptotic BER analysis under different AT regimes.

The rest of the paper is organized as follows. In Section II, the Tx and channel models with general assumptions are briefly presented. In Section III, Rx models for the considered correlated FSO-MIMO system both in the absence

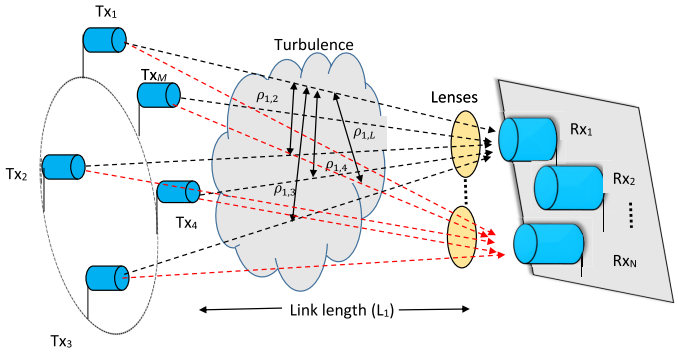

FIGURE 1. Demonstrative diagram of arbitrarily correlated FSO-MIMO system.

and presence of the ASE noise are presented followed by the derivation of analytical BER results. Further, we also perform asymptotic BER analysis at high SNR to get some intuition about the impact of correlation and the ASE noise on the diversity order G_d, coding gain G_c, and loss in coding gain $\Delta\ G_c^L$ in Section IV. Numerical results are presented and discussed in Section V. In Section VI, an experimental set-up is developed for a 2×1 correlated FSO system with RC. Finally in Section VII, we present concluding remarks based on the numerical results and observations.

II. PRELIMINARIES

Let us consider an IM/DD FSO-MIMO system consisting of M-Tx lasers, and N-Rx apertures, as shown in Fig. 1. We assume a FSO-MIMO system, where the lasers at the transmitting end are closely spaced; and similarly, the Rx apertures are also closely spaced, thus resulting in channels with arbitrary correlation [4], [16]. The information bit stream, converted into a non-return-to-zero (NRZ) OOK format with RC, is used for IM of multiple Txs for transmission over an arbitrarily correlated $\Gamma\Gamma$ AT channel [30].

A. CHANNEL MODEL

In this paper, we characterize the fading behaviour of the FSO channel using the $\Gamma\Gamma$ turbulence model. Let $I_{n,m}$ denotes the received signal irradiance at n-th Rx from m-th Tx, which is given as:

$$I_{n,m} = I_0 h_{n,m}, \tag{1}$$

where I_0 is the received irradiance through the clear air channel, $h_{n,m}$ represents the correlated channel gain between the m-th Tx-laser and the n-th Rx-aperture with $1 \leq m \leq M$ and $1 \leq n \leq N$, which is modelled as $\Gamma\Gamma$ RV. As a result of the linear relation between $I_{n,m}$ and $h_{n,m}$ in (1), $I_{n,m}$ also follows the $\Gamma\Gamma$ distribution with arbitrary correlation.

B. GENERAL ASSUMPTIONS

In order to simplify the generalized discussion for FSO-MIMO channel, let us consider $\mathbf{H}$ be an $N \times M$ arbitrarily correlated channel gain matrix with $h_{n,m} \in \mathbf{H}$. Vectorization of matrix $\mathbf{H}$, i.e., $\mathbf{h} = \text{vec}(\mathbf{H})$ gives a vector of size $NM \times 1$ with MN $\Gamma\Gamma$ distributed channel coefficients. Let us represent them by a compact notation h_i, $i = 1, 2, \ldots, MN$ without loss of generality. The correlated $\Gamma\Gamma$ RVs h_is for a MIMO channel can be generated as a product of two sets of Gamma RVs w_is and u_is, which arises from large-scale and small-scale eddies, respectively [16]. Further, ρ_w and ρ_u denote the correlation coefficients of large-scale and small-scale eddies, respectively and $\rho_{i,j}$ represents the effective correlation coefficient between the i-th and j-th sub-channels, $j = 1, 2, \ldots, MN$. Since the large-scale and small-scale fadings are considered to be independent according to the $\Gamma\Gamma$ model, $\rho_{i,j}$ can be given by [15]:

$$\rho_{i,j} = \frac{\sqrt{\alpha_i \alpha_j}\rho_u + \sqrt{\beta_i \beta_j}\rho_w + \rho_w \rho_u}{\sqrt{\alpha_i + \beta_i + 1}\sqrt{\alpha_j + \beta_j + 1}}, \tag{2}$$

where α_i and β_i are the turbulence parameters associated with i-th sub-channel, which denote the effective numbers of large-scale and small-scale eddies [1], respectively and their effective sizes vary from the inner-scale to the outer-scale of turbulence denoted by l_0 and L_0, respectively. In the case of plane wave (link length $\geq$ 1 Km) propagation with l_0 close to 0, i.e., a zero inner scale condition, the AT parameters of α_i and β_i can be obtained using [31]:

$$\alpha_i = \left(\exp\left[\frac{0.49\sigma_{R_i}^2}{(1 + 1.11\sigma_{R_i}^{12/5})^{7/6}} \right] - 1 \right)^{-1}, \tag{3}$$

$$\beta_i = \left(\exp\left[\frac{0.51\sigma_{R_i}^2}{(1 + 0.69\sigma_{R_i}^{12/5})^{5/6}} \right] - 1 \right)^{-1}, \tag{4}$$

where $\sigma_{R_i}^2$ is the Rytov variance of i-th sub-channel, which represents irradiance fluctuations associated with AT, given by $\sigma_{R_i}^2 = 1.23 C_{n_i}^2 k^{7/6} L_1^{11/6}$ for the plane wave, where L_1 is the link length, $C_{n_i}^2$ is the refractive index structure parameter of the i-th sub-channel, and $k = 2\pi/\lambda$ is the wave-number. Morever, for spherical wave propagation, the AT parameters

are given as [31]:

$$\alpha_i = \left(\exp\left[\frac{0.49\sigma_{R_i}^2}{(1+0.56\sigma_{R_i}^{12/5})^{7/6}} \right] - 1 \right)^{-1}, \quad (5)$$

$$\beta_i = \left(\exp\left[\frac{0.51\sigma_{R_i}^2}{(1+0.69\sigma_{R_i}^{12/5})^{5/6}} \right] - 1 \right)^{-1}, \quad (6)$$

where $\sigma_{R_i}^2 = 0.5C_{n_i}^2 k^{7/6} L_1^{11/6}$.

In order to generate correlated $\Gamma\Gamma$ RVs for a given $\rho_{i,j}$, the challenge is to find appropriate values of ρ_w and ρ_u using (2) for the considered channel. This is because it can be observed from (2) that, for a given $\rho_{i,j}$ there are an infinite number of possible solutions. However, in [32, Section 5], the specific criteria for setting large and small-scale correlation coefficients based on the scintillation theory, were proposed, which can be used to easily determine the parameters ρ_w and ρ_u.

Before setting ρ_w and ρ_u, let us first define the three scale sizes z_1, z_2, and z_3 as the spatial coherence radius r_0, the first Fresnel zone $\sqrt{L_1/k}$, and the scattering disk size L_1/kr_0, respectively where r_0 depends on L_1 and C_n^2, and given as $r_0 = \left(1.455(2\pi/\lambda)^2 C_n^2 L_1\right)^{-3/5}$ for plane wave and $r_0 = \left(0.555(2\pi/\lambda)^2 C_n^2 L_1\right)^{-3/5}$ for spherical wave. For strong AT, intensity fluctuations arising from small-scale eddies is averaged; thus $\rho_u \approx 0$. Moreover, under weak-to-moderate AT conditions, when $z_1 > z_2 > z_3$, generally the proposed solution is to set $\rho_w = \rho_u$. However, for the value of ρ obtained with this solution, we can reasonably set $\rho_u = 0$ in (2) to obtain the value of ρ_w as an equivalent solution for $\rho = \rho_w = \rho_u$.

Therefore, in this work, we consider RVs u_is to be independent, and the RVs arising from large-scale eddies w_is to be arbitrarily correlated. The correlation between w_is and w_js is defined by the correlation matrix Σ, of size $MN \times MN$ with $\Sigma_{i,j} \equiv 1$ for $i = j$ and $\Sigma_{i,j} \equiv \rho_{i,j}$ for $i \neq j$, and $\Sigma_{i,j} \in \Sigma$. $\rho_{i,j}$ is defined as:

$$\rho_{i,j} \triangleq \frac{\mathrm{cov}(w_i, w_j)}{\sqrt{\mathrm{var}(w_i)\mathrm{var}(w_j)}}, \quad (7)$$

where $0 \leq \rho_{i,j} < 1$, $\mathrm{cov}(\cdot)$ and $\mathrm{var}(\cdot)$ denote the covariance and variance, respectively [16], [33]–[35]. According to [36], $\rho_{i,j}$ also depends on the transversal distance between the i-th and j-th apertures $d_r^{(i,j)}$ and the spatial coherence radius r_0, which can be expressed as:

$$\rho_{i,j} = \exp\left(-\left(d_r^{(i,j)}/r_0\right)^{5/3} \right). \quad (8)$$

For a given separation among two apertures, the existing correlation level can be calculated using (8).

C. STATISTICS OF CORRELATED $\Gamma\Gamma$ AT MODEL

The joint pdf of $L = MN$ $\Gamma\Gamma$ RVs h_is with arbitrary correlation and identical distribution is given by (9) (given on the bottom of this page) [16], [37]. In this expression, $|\cdot|$, $K_v(\cdot)$, and $\Gamma(\cdot)$ denote the determinant, modified Bessel function of the second kind of order v [38] and Gamma function, respectively; $\Omega = \mathrm{E}[h_i]/\alpha$, where $\mathrm{E}(\cdot)$ denotes the expectation and α and β are the AT parameters. Further, $\mathbf{W}$ represents the inverse of correlation matrix Σ (i.e., $\mathbf{W} = \Sigma^{-1}$), $w_{i,j}$s denote the elements of $\mathbf{W}$, $\delta_j \triangleq ((\alpha + m_j + \beta)/2) - 1$, $\eta_j \triangleq ((\alpha + m_j - \beta)/2)$ with $m_j = i_j$ for $j = 1$, $m_j = i_{L-1}$ for $j = L$ and $m_j = i_{j-1} + i_j$ for $j = 2, 3, \ldots, (L-1)$ [16]. Note that, (9) is valid only when the matrix $\mathbf{W}$ follows the tridiagonal property. However, the inverse of matrix Σ is not always tridiagonal for all practical correlation models. Therefore, in this paper we will use Green's matrix approximation of Σ in the analysis [35].

D. SUM OF ARBITRARILY CORRELATED AND NON-IDENTICALLY DISTRIBUTED $\Gamma\Gamma$ RVS

Let us consider a set of L correlated $\Gamma\Gamma$ RVs $[h_1, \ldots, h_L]$ and their sum $h_{\mathrm{sm}} = \sum_{i=1}^{L} h_i$. Note that, h_i is the product of two Gamma RVs, i.e., $[h_1, \ldots, h_L] = [u_1 w_1, \ldots, u_L w_L]$. It is assumed that, the vector $[u_1, \ldots, u_L]$ contains independent and identically distributed Gamma RVs with the parameter β [14], whereas $[w_1, \ldots, w_L]$ corresponds to the vector containing L arbitrarily correlated non-identical Gamma RVs with parameters[1] α_i and $\Omega_i = \mathrm{E}[w_i]/\alpha_i$ [16]. The Karhunen-Loeve expansion is employed to decorrelate the arbitrarily correlated, non-identical, Gamma distributed RVs w_is to obtain a new set of independent and non-identically distributed Gamma RVs [40]. Then, by expressing the sum of a new set of independent Gamma RVs as a nested finite weighted sum of Gamma RVs, a closed-form expression for the pdf of h_{sm} is obtained by employing the transformation of RVs. But, before discussing the pdf of h_{sm}, let us take into account the following assumptions, which are applicable to this pdf [39]:

- Without loss of generality it is assumed that, the AT parameters lie in increasing order, i.e., $\alpha_1 \leq \alpha_2 \leq \ldots \leq \alpha_L$.
- Let $z_i = [z_{i,1}, z_{i,2} \ldots z_{i,2\alpha_i}]^T$ is a vector of size $2\alpha_i \times 1$, which contains independent and identically distributed Gaussian RVs, $\{z_{i,k}\}_{k=1}^{2\alpha_i}$, with $\mathrm{E}[z_{i,k}^2] = \Omega_i/2$.

[1]Note that, the AT parameter α_i is considered to be a positive integer [39].

$$f_{h_1 \ldots . h_L}(h_1, \ldots, h_L) = \frac{2^L \mid \mathbf{W} \mid^{\alpha}}{\Gamma(\alpha)\Gamma(\beta)^L} \sum_{i_1, \ldots, i_{L-1}=0}^{\infty} \left(\frac{\beta}{\Omega}\right)^{\frac{L(\alpha+\beta)}{2} + \sum_{j=1}^{L-1} i_j} \prod_{j=1}^{L} \frac{h_j^{\delta_j}}{w_{j,j}^{\eta_j}} \times K_{2\eta_j}\left(2\sqrt{\frac{\beta w_{j,j}}{\Omega} h_j}\right) \prod_{n=1}^{L-1} \left[\frac{\mid w_{n,n+1} \mid^{2i_n}}{i_n! \Gamma(\alpha + i_n)}\right] \quad (9)$$

- Let $z = [z_1^T z_2^T \cdots z_L^T]^T$ be another vector of order $D \times 1$ with $D = \sum_{i=1}^{L} 2\alpha_i$ and λ_i is a set of L distinct eigenvalues of the covariance matrix $K_{z_{i,j}^{(k,l)}} = \mathrm{E}[z_{i,k} z_{j,l}]$, which can be given as:

$$K_{z_{i,j}^{(k,l)}} = \begin{cases} \Omega_i/2 & \text{if } i = j \text{ and } k = l \\ \rho_{i,j}^{(z)} \sqrt{\Omega_i \Omega_j}/2 & \text{if } i \neq j \\ & \text{and } k = l = 1, 2 \\ & , .., 2\min\{\alpha_i, \alpha_j\} \\ 0 & \text{otherwise,} \end{cases} \quad (10)$$

  where $\rho_{i,j}^{(z)}$ denotes the correlation among the elements of z.
- Moreover, μ_i is the algebraic multiplicity of each λ_i, which satisfies $\sum_{i=1}^{L} \mu_i = D$.

Based on the aforementioned assumptions and discussions, pdf of h_{sm} can be accurately approximated as the weighted sum of independent $\Gamma\Gamma$ RVs[2] with parameters $\alpha_i = \mu_i/2$ and $\Omega_i = 4\lambda_i/\mu_i$ (where μ_i and λ_i are already defined under the assumptions), as given by [16], [39]:

$$f_{h_{\mathrm{sm}}}(h_{\mathrm{sm}}) = \sum_{i=1}^{L} \sum_{j'=1}^{\alpha_i} 2\, \Xi_L(i, j', \{\alpha_q\}_{q=1}^{L}, \{\Omega_q\}_{q=1}^{L}) \times \frac{(L\beta)^{\frac{L\beta+j'}{2}} h_{\mathrm{sm}}^{\frac{L\beta+j'}{2}-1}}{\Gamma(j')\Gamma(L\beta)(\Omega_i)^{\frac{L\beta+j'}{2}}} K_{j'-L\beta}\left(2\sqrt{\frac{L\beta h_{\mathrm{sm}}}{\Omega_i}}\right), \quad (11)$$

where the weights $\Xi_L(i, j', \{\alpha_q\}_{q=1}^{L}, \{\Omega_q\}_{q=1}^{L})$ can be calculated using the recursive formula of [39, Eq. (8)].

III. PERFORMANCE ANALYSIS OF RC OVER CORRELATED ΓΓ AT

In this section, we will describe the Rx models of the considered correlated FSO-MIMO system with RC, with and without the erbium-doped fiber amplifier (EDFA) and associated ASE noise followed by the derivation of their analytical BER results.

A. FSO-MIMO WITH NO OPTICAL PRE-AMPLIFIER

1) RECEIVER MODEL

The equal gain combining is performed to obtain the received electrical signal at the Rx with no optical pre-amplification as:

$$r = \sqrt{E_b} \sum_{n=1}^{N} \sum_{m=1}^{M} h_{n,m} x + \sum_{n=1}^{N} e_n, \quad (12)$$

where $E_b = \frac{\eta^2 I_0^2}{M^2 N^2}$, η represents an optical-to-electrical conversion coefficient, I_0 is the light intensity received at the photo-detector without considering the channel effect, $x \in \{0, 1\}$ denotes the transmitted symbol and e_n is the total noise at the Rx, which is modelled as an additive white Gaussian noise (AWGN) with zero mean and variance of $N_0/2$. Moreover, the factor $1/MN$ is used to normalize the total transmit and receive power levels, in order to keep the total radiated power of MIMO the same as the SISO. Note that, we have employed an ML detection scheme at the Rx.

2) AVERAGE BER EVALUATION

For the given input-output (I/O) relation of the MIMO system (12), the instantaneous SNR at the Rx with no pre-amplification for RC is given by [10]:

$$\gamma = \frac{\eta^2 I_0^2}{2M^2 N^2 N_0} \left(\sum_{n=1}^{N} \sum_{m=1}^{M} h_{n,m} \right)^2. \quad (13)$$

Note that, the average SNR is denoted as $\bar{\gamma} = (\eta^2 I_0^2)/N_0$ and without the loss of generality, it is assumed that the average irradiance is normalized. The conditional BER of RC over $\Gamma\Gamma$ AT with arbitrary correlation can be given as:

$$P_{e|h} = Q(\sqrt{\gamma}) = Q\left(\sqrt{\frac{E_b}{2N_0}} \sum_{n=1}^{N} \sum_{m=1}^{M} h_{n,m} \right). \quad (14)$$

To derive the BER of FSO-MIMO with RC, we need to average (14) over the pdf of MN correlated $\Gamma\Gamma$ RVs, i.e., the pdf of $h_{\mathrm{sm}} = \sum_{n=1}^{N} \sum_{m=1}^{M} h_{n,m}$. The exact pdf of h_{sm} remains unknown, however, the proposed problem can be made analytically tractable by employing the approximate pdf described in Section II-E, with correlated physical diversity sub-channels being transformed into independent virtual sub-channels. By using the relation $Q(x) \approx \frac{1}{2}\exp(-x^2/2)$ in (14), substituting and considering η and I_0 to be 1, the average BER can be obtained from:

$$P_e \approx \frac{1}{2} \int_0^{\infty} \exp\left(\frac{-h_{\mathrm{sm}}^2}{4N_0 M^2 N^2} \right) f_{h_{\mathrm{sm}}}(h_{\mathrm{sm}}) dh_{\mathrm{sm}}, \quad (15)$$

where $f_{h_{\mathrm{sm}}}(h_{\mathrm{sm}})$ is as given in (11).

Substituting (11) in (15), followed by some mathematical manipulations and employing [41, Eq.(2.24.3/1)], the BER of the FSO-MIMO under $\Gamma\Gamma$ AT with arbitrary correlation is obtained in the form of:

$$P_e \approx \frac{1}{8\pi} \sum_{i=1}^{L} \sum_{j'=1}^{\alpha_i} \Xi_L(i, j', \{\alpha_q\}_{q=1}^{L}, \{\Omega_q\}_{q=1}^{L}) \times \frac{(L\beta)^{\frac{L\beta+j'}{2}}}{\Gamma(j')\Gamma(L\beta)(\Omega_i)^{\frac{L\beta+j'}{2}}} \left(\frac{1}{4N_0 M^2 N^2} \right)^{\frac{-L\beta-j'}{4}} \times G_{1,4}^{4,1}\left(\left(\frac{L\beta}{\Omega_i} \right)^2 \frac{4N_0 M^2 N^2}{2^4} \middle| \begin{matrix} \frac{4-L\beta-j'}{4} \\ b \end{matrix} \right), \quad (16)$$

where $L = MN$, $b = \left[\frac{j'-L\beta}{4}, \frac{j'-L\beta+2}{4}, \frac{L\beta-j'}{4}, \frac{L\beta-j'+2}{4}\right]$. Let us make the following remarks on the derived BER expression in (16):

[2]The pdf given in (11) is applicable to the scenario when correlation among the large-scale eddies dominates the correlation among the small-scale eddies. Nevertheless, the sum of correlated $\Gamma\Gamma$ RVs, when both the small and large-scale eddies are contributing to the effective correlation can also be derived easily by following the procedure given in [39].

- The derived closed-form BER expression consists of finite nested summations and also the weight coefficients can be easily evaluated by using the recursive formula given in [39, Eq. (8)]. It makes the BER result evaluation very easy and fast.
- Moreover, the derived expression is very much generalized as it is valid for the FSO-MIMO system with non-identical links, arbitrary correlation, and wide range of AT regime.[3]

B. BER OF RC OVER CORRELATED $\Gamma\Gamma$ AT WITH EDFA PRE-AMPLIFIER

1) RECEIVER MODEL

At the Rx, N plano-convex lenses and collimators are used to couple the received optical signal into the single mode fibers (SMF) the output of which are combined and then amplified. Note, the pre-amplifier introduces an additional noise of ASE, which is modeled as zero mean Gaussian noise with two-sided power spectral density of $N_0/2$, with $N_0 = N_{\text{sp}}h'\nu(G-1)$. Here h' is Planck's constant, ν is the optical center frequency, G is the amplifier gain, and N_{sp} is spontaneous emission factor [20], [42]. It is assumed that, the optical gain is sufficiently high such that the ASE noise is the dominant source compared with the shot and thermal noise sources at the Rx [20], [22], [25], [42]. Prior to square law detection, the received optical signal with noise is passing through a band-pass filter in order to improve the SNR (i.e., reduce the noise). Let us assume that, the dimensionality of the space of finite energy signals with a bandwidth B and the time spread T is an even integer of $2M_1$. The filtered noise process at the photo-detector over T and orthonormal functions $\phi_{i'}$ can be denoted as $\sum_{i'=1}^{2M_1} n_{i'}\phi_{i'}(t)$, where $n_{i'}$ is Gaussian RV with zero mean and variance $N_0/2$. The information signal with the energy $E = \sum_{i'=1}^{2M_1} s_{i'}^2$ at the photo-detector can also be represented in the same orthonormal basis as $\sum_{i'=1}^{2M_1} s_{i'}\phi_{i'}(t)$. The generated photo-current $I = \left(\sum_{i'=1}^{2M_1}\left(\sum_{n=1}^{L} h_n s_{i'} + n_{i'}\right)\phi_{i'}(t)\right)^2$, where $L = MN$. Equalization is performed on the electrical signal and then it is averaged over a one-bit duration to obtain the decision variable, which is given as:

$$y = \sum_{i'=1}^{2M_1}\Big(\sum_{n=1}^{L} h_n s_{i'} + n_{i'}\Big)^2 = \sum_{i'=1}^{2M_1}\big(h_{\text{sm}}s_{i'} + n_{i'}\big)^2, \quad (17)$$

where y follows the Chi-square distribution [20]. If the binary 1 is transmitted (i.e., signal present), then the statistical behaviour of y can be more accurately described as non-central Chi-square distribution with $2M_1$ degrees of freedom:

$$f_y(y \mid h_{\text{sm}}, x=1) = \frac{(h_{\text{sm}})^2}{N_0}\Big(\frac{y}{E}\Big)^{\frac{M_1-1}{2}} e^{-\frac{(y+E)h_{\text{sm}}^2}{N_0}} I_{M_1-1}\left(\frac{2h_{\text{sm}}^2\sqrt{yE}}{N_0}\right), \quad (18)$$

[3]Note that, the BER expression reported in [17, Eq. (12)], which was derived for FSO-MISO system with constant correlation, can be considered as a special case of (16).

where E is the bit energy and $I_v(x)$ is the modified Bessel function of the first kind of order v.

If the binary 0 is transmitted (i.e., no signal) with $E = 0$, then y follows central Chi-square distribution given as:

$$f_y(y \mid h_{\text{sm}}, x=0) = \Big(\frac{h_{\text{sm}}^2}{N_0}\Big)^{M_1}\frac{y^{M_1-1}}{(M_1-1)!}e^{-\frac{yh_{\text{sm}}^2}{N_0}}, \quad (19)$$

where $(\cdot)!$ represents the factorial operation.

2) CONDITIONAL BER

In order to decide whether the binary 1 or 0 has been received, threshold based detection is adopted using $y \underset{0}{\overset{1}{\gtrless}} y_{\text{th}}$ to compare the decision variable with a threshold level y_{th}. Based on this decision, there are two possible errors: i) $P(e \mid h_{\text{sm}}, 0 \to 1)$: binary 1 is detected when 0 is transmitted. ii) $P(e \mid h_{\text{sm}}, 1 \to 0)$: binary 0 is detected when 1 is transmitted, where, we have

$$P(e \mid h_{\text{sm}}, 0 \to 1) = \int_{y_{\text{th}}}^{\infty} f_y(y \mid h_{\text{sm}}, x=0)dy. \quad (20)$$

and

$$P(e \mid h_{\text{sm}}, 1 \to 0) = \int_{0}^{y_{\text{th}}} f_y(y \mid h_{\text{sm}}, x=1)dy. \quad (21)$$

Substituting (19) in (20) and employing [43, Eq. (3.381/3)], we have:

$$P(e \mid h_{\text{sm}}, 0 \to 1) = \frac{1}{(M_1-1)!}\Gamma\left(M_1, \frac{h_{\text{sm}}^2 y_{\text{th}}}{N_0}\right). \quad (22)$$

Further, by replacing $I_v(x)$ with its series form (given in [43, Eq. (8.445)]) in (18), then substituting it in (21), and following some mathematical manipulations, P_1 can be expressed as:

$$P(e \mid h_{\text{sm}}, 1 \to 0) = \sum_{k=0}^{\infty}\Big(\frac{h_{\text{sm}}^2}{N_0}\Big)^k \frac{E^k e^{-Eh_{\text{sm}}^2/N_0}}{\Gamma(k+M_1)k!} \times \gamma\left(k+M_1, \frac{y_{\text{th}}h_{\text{sm}}^2}{N_0}\right), \quad (23)$$

where $\gamma(\cdot,\cdot)$ is the lower incomplete Gamma function. Now, for the equiprobable input signals, the conditional error probability can be obtained using $P_{e|h_{\text{sm}}} = \frac{1}{2}(P(e \mid h_{\text{sm}}, 0 \to 1) + P(e \mid h_{\text{sm}}, 1 \to 0))$.

3) AVERAGE BER CALCULATION

Having obtained the conditional error probability, the average BER can be evaluated by averaging $P_{e|h_{\text{sm}}}$ over the MIMO fading channel h_{sm} as given by:

$$\begin{aligned} P_e &= \int_0^{\infty} P_{e|h_{\text{sm}}} f_{h_{\text{sm}}}(h_{\text{sm}})dh_{\text{sm}} \\ &= \frac{1}{2}\Bigg(\underbrace{\int_0^{\infty} P(e \mid h_{\text{sm}}, 0 \to 1) f_{h_{\text{sm}}}(h_{\text{sm}})dh_{\text{sm}}}_{I_1} \\ &\quad + \underbrace{\int_0^{\infty} P(e \mid h_{\text{sm}}, 1 \to 0) f_{h_{\text{sm}}}(h_{\text{sm}})dh_{\text{sm}}}_{I_2}\Bigg). \end{aligned} \quad (24)$$

To simplify the analysis, let us first calculate the integral I_1 of (24) by substituting (11) and (22) in I_1 and using the series representation of Gamma function as given by:

$$\Gamma(a,x) = e^{-x}\sum_{p=0}^{a-1}\frac{(a-1)!}{p!}x^p. \tag{25}$$

Employing the above series, replacing the modified Bessel function of the second kind by a Meijer-G function in $f_{h_{\rm sm}}(h_{\rm sm})$, followed by some mathematical substitutions, and then employing [41, Eq. (2.24.3/1)], the integral I_1 is solved to obtain:

$$P_e^{(1)} = \sum_{p=0}^{M_1-1}\sum_{i=1}^{L}\sum_{j'=1}^{\alpha_i}\frac{\Xi_L(i,j')(L\beta)^{\frac{L\beta+j'}{2}}}{4\pi p!\Gamma(j')\Gamma(L\beta)(\Omega_i)^{\frac{L\beta+j'}{2}}} \times \left(\frac{y_{\rm th}}{N_0}\right)^{-\frac{(L\beta+j')}{4}} G_{1,4}^{4,1}\left(\left(\frac{L\beta}{\Omega_i}\right)^2\frac{N_0}{y_{\rm th}2^4}\middle|\begin{matrix}\frac{4-4p-L\beta-j'}{4}\\ \\ b\end{matrix}\right), \tag{26}$$

where **b** is defined in Section III-A.2.

The integral I_2 can be solved by employing a series representation of $\gamma(\cdot,\cdot)$, given as [43, Eq. (8.354/1)], in (23) and then substituting it and (11) in the integral I_2 to obtain:

$$I_2 = \int_0^\infty \sum_{k,n=0}^{\infty}\sum_{i=1}^{L}\sum_{j'=1}^{\alpha_i}\Psi(y_{\rm th},\alpha_i,\Omega_i)h_{\rm sm}^{2D}e^{-\frac{Eh_{\rm sm}^2}{N_0}} \times G_{0,2}^{2,0}\left(\frac{L\beta h_{\rm sm}}{\Omega_i}\middle|\begin{matrix}\cdot\ ,\ \cdot\\ \\ \frac{j'-L\beta}{2},\ \frac{L\beta-j'}{2}\end{matrix}\right)dh_{\rm sm}, \tag{27}$$

where $D = 2k + M_1 + n + \frac{L\beta+j'}{4} - \frac{1}{2}$ and

$$\Psi(y_{\rm th},\alpha_i,\Omega_i) = \frac{E^k}{N_0^k\Gamma(k+M_1)k!}\frac{(-1)^n}{n!(k+M_1+n)} \times \left(\frac{y_{\rm th}}{N_0}\right)^{k+M_1+n}\frac{\Xi_L(i,j')(L\beta)^{\frac{L\beta+j'}{2}}}{\Gamma(j')\Gamma(L\beta)(\Omega_i)^{\frac{L\beta+j'}{2}}}. \tag{28}$$

The integral in (27) can be solved by carrying out transformation of RVs and then employing [41, Eq. (2.24.3/1)] to obtain:

$$P_e^{(2)} = \sum_{k,n=0}^{\infty}\sum_{i=1}^{L}\sum_{j'=1}^{\alpha_i}\left(\frac{E}{N_0}\right)^{-2k-M_1-n-\frac{L\beta}{4}-\frac{j'}{4}} \times \frac{\Psi(y_{\rm th},\alpha_i,\Omega_i)}{4\pi}G_{1,4}^{4,1}\left(\left(\frac{L\beta}{\Omega_i}\right)^2\frac{N_0}{E2^4}\middle|\begin{matrix}\Phi_1\\ \\ b\end{matrix}\right), \tag{29}$$

where $\Phi_1 = (1-2k-M_1-n-L\beta/4-j'/4)$.

Finally, the average BER of the correlated FSO-MIMO system with RC in the presence of ASE noise can be obtained using $P_e = 1/2(P_e^{(1)} + P_e^{(2)})$ by substituting (26) and (29) in (24).

Let us make some remarks on the derived expression for BER of the considered correlated system with the ASE noise:

- The BER expression derived for the considered system with pre-amplifier is quite simple and can be easily implemented, since (26) consists of only finite weighted summations and the power series in (29) converge very fast at $k, n \approx 8-10$. The Cauchy ratio test [38], [44] can be adopted to prove the convergence of the power series in (29).
- The derived BER result is very generalized and valid for practical scenarios where links are not necessarily identical, correlation is arbitrary and also the ASE noise is dominant.

IV. ASYMPTOTIC BER ANALYSIS

It is not possible to get any intuition of the diversity order of the system from (16), (26), and (29). Therefore, for a better understanding of the system's performance behaviour, the asymptotic BER analysis at high SNR is performed in this section. Both G_c and G_d are the two well known parameters, which are used to quantify the BER performance at high SNR. The parameter G_c contributes to the horizontal shift of BER plots against SNR on a log-log scale, i.e., difference between the SNR levels required in two plots to reach the same value of BER. Whereas, G_d specifies the slope of decay of the plots at very high values of SNR.

A. DIVERSITY ANALYSIS OF FSO-MIMO SYSTEM WITHOUT EDFA

To perform asymptotic BER analysis for the FSO-MIMO system with no EDFA, let us rewrite Meijer-G function in (16) in terms of the generalized hypergeometric function (using Slater's theorem [41]) to obtain:

$$\tilde{P}_e \approx \frac{1}{8\pi}\sum_{i=1}^{L}\sum_{j'=1}^{\alpha_i}\Xi_L(i,j',\{\alpha_q\}_{q=1}^L,\{\Omega_q\}_{q=1}^L) \times \frac{(L\beta)^{\frac{L\beta+j'}{2}}}{\Gamma(j')\Gamma(L\beta)(\Omega_i)^{\frac{L\beta+j'}{2}}}\left(\frac{\bar{\gamma}}{4M^2N^2}\right)^{\frac{-L\beta-j'}{4}} \times \left[\sum_{h=1}^{4}\prod_{k=1}^{4}\Gamma(b_k-b_h)^*\Gamma(1+b_h-\frac{4-L\beta-j'}{4}) \times \zeta^{b_h}{}_1F_3\left((-1)^{-4}\zeta\middle|\begin{matrix}1+b_h-\frac{4-L\beta-j'}{4}\\ \\ (1+b_h-b_q)^*\end{matrix}\right)\right], \tag{30}$$

where $\zeta = \left(\frac{L\beta}{\Omega_i}\right)^2\frac{4M^2N^2}{2^4\bar{\gamma}}$, $b_k, b_h, b_q \in b$ with $k, h, q \in \{1,2,3,4\}$ and $\bar{\gamma}$ is the average SNR. The notation $\Gamma(z)^*$ signifies that $\Gamma(z) = 1$ for $z \le 0$, and the asterisk sign in the argument of the hypergeometric function indicates to ignore the terms with $h = q$. At high SNR, the hypergeometric function in (30) tends to unity, i.e., ${}_1F_3(\cdot) \to 1$ [38], which results in a simplified asymptotic BER expression. After some rearrangements and simplification in (30),

we have:

$$\tilde{P}_e \approx \frac{1}{8\pi}\sum_{i=1}^{L}\sum_{j'=1}^{\alpha_i}\Xi_L(i,j',\{\alpha_q\}_{q=1}^{L},\{\Omega_q\}_{q=1}^{L}) \times \frac{(L\beta)^{\frac{L\beta+j'}{2}}}{\Gamma(j')\Gamma(L\beta)(\Omega_i)^{\frac{L\beta+j'}{2}}}\left(\frac{\bar{\gamma}}{4M^2N^2}\right)^{\frac{-L\beta-j'}{4}} \times\left[\sum_{h=1}^{4}\prod_{k=1}^{4}\left(\left(\frac{L\beta}{\Omega_i}\right)^2\frac{4M^2N^2}{2^4\bar{\gamma}}\right)^{b_h} \times\Gamma(b_k-b_h)^*\Gamma(1+b_h-\frac{4-L\beta-j'}{4})\right]. \quad (31)$$

It is well established in the literature that, the asymptotic BER at high SNR is given by [45]:

$$\tilde{P}_e \approx (G_c\bar{\gamma})^{-G_d}. \quad (32)$$

The asymptotic value of the BER at high SNR is dominated by the term that corresponds to the smallest exponent of average SNR $\bar{\gamma}$ in the asymptotic BER expression [45]. However, all the terms corresponding to the summations with indices i and j' must be present in (31), because the weighting coefficients, $\Xi_L(i,j')$, incorporate the effect of correlation and cannot be ignored (as it is obtained from the eigen-values of the correlation matrix). It can be observed from (31) that, each summation term will have one of the four terms from the vector $\{b_h+(L\beta+j')/4\}\in\{\frac{j'}{2},\frac{j'+1}{2},\frac{L\beta}{2},\frac{L\beta+1}{2}\}$, as the exponent of average SNR $\bar{\gamma}$. For $\alpha > \beta$, then within the summation with the index h, only the term corresponding to b_3 will dominate (i.e., the smallest exponent). However, for $\alpha < \beta$, both terms corresponding to b_1 and b_2 will contribute.

Based on the aforementioned discussions, the diversity order of the considered system without EDFA is given as:

$$G_d = L\min\{\frac{\alpha_1}{2},\frac{\beta}{2}\}. \quad (33)$$

B. DIVERSITY ANALYSIS OF FSO-MIMO SYSTEM WITH EDFA

As mentioned in Section III-B.3, the BER expression of FSO-MIMO system with EDFA is obtained from (26) and (29) using $P_e = 1/2(P_e^{(1)}+P_e^{(2)})$; therefore, the corresponding asymptotic BER expression can be obtained from $\tilde{P}_e = 1/2(\tilde{P}_e^{(1)}+\tilde{P}_e^{(2)})$. For a better understanding of the asymptotic BER analysis, let us study the asymptotic behaviour of two components of the BER expression (Eqs. (26) and (29)) one by one. In order to obtain $\tilde{P}_e^{(1)}$, Meijer-G function in (26) is rewritten in terms of the generalized hypergeometric function to obtain:

$$\tilde{P}_e^{(1)} = \sum_{p=0}^{M_1-1}\sum_{i=1}^{L}\sum_{j'=1}^{\alpha_i}\frac{\Xi_L(i,j')(L\beta)^{\frac{L\beta+j'}{2}}}{4\pi p!\Gamma(j')\Gamma(L\beta)(\Omega_i)^{\frac{L\beta+j'}{2}}} \times\left(y_{\text{th}}\bar{\gamma}\right)^{-\frac{(L\beta+j')}{4}}\sum_{h=1}^{4}\prod_{m=1}^{4}\Gamma(b_m-b_h)^* \times\Gamma\left(1+b_h-(\frac{4-4p-L\beta-j'}{4})\right)\left((\frac{L\beta}{\Omega_i})^2\frac{1}{y_{\text{th}}2^4\bar{\gamma}}\right)^{b_h} \times{}_1F_3\left((-1)^{-4}(\frac{L\beta}{\Omega_i})^2\frac{1}{y_{\text{th}}2^4\bar{\gamma}}\middle|\begin{matrix}1+b_h-\frac{4-4p-L\beta-j'}{4}\\(1+b_h-b_q)^*\end{matrix}\right), \quad (34)$$

where $b_m, b_h, b_q \in b$ with $m,h,q \in \{1,2,3,4\}$ and $\bar{\gamma}$ is the average SNR. As already discussed, at very high SNR we have ${}_1F_3(\cdot)\to 1$; and the Gamma function with asterisk sign signifies that, for $(b_m - b_h) \le 0$, the contribution of Gamma function is ignored by setting $\Gamma(b_m-b_h)^*=1$, which gives:

$$\tilde{P}_e^{(1)} = \sum_{p=0}^{M_1-1}\sum_{i=1}^{L}\sum_{j'=1}^{\alpha_i}\frac{\Xi_L(i,j')(L\beta)^{\frac{L\beta+j'}{2}}}{4\pi p!\Gamma(j')\Gamma(L\beta)(\Omega_i)^{\frac{L\beta+j'}{2}}} \times\left(y_{\text{th}}\bar{\gamma}\right)^{-\frac{(L\beta+j')}{4}}\sum_{h=1}^{4}\prod_{m=1}^{4}\Gamma(b_m-b_h)^* \times\Gamma\left(1+b_h-(\frac{4-4p-L\beta-j'}{4})\right)\left((\frac{L\beta}{\Omega_i})^2\frac{1}{y_{\text{th}}2^4\bar{\gamma}}\right)^{b_h}. \quad (35)$$

Now, in order to obtain the second asymptotic component of the BER, i.e., $\tilde{P}_e^{(2)}$ from (29), the power series in (29) is considered only at $k,n=0$. Here also, Meijer-G function is expressed in terms of the generalized hypergeometric function and at high SNR we have ${}_1F_3(\cdot)\to 1$, which results in:

$$\tilde{P}_e^{(2)} = \sum_{i=1}^{L}\sum_{j'=1}^{\alpha_i}\frac{y_{\text{th}}^{M_1}}{\Gamma(M_1)M_1}\frac{\Xi_L(i,j')(L\beta)^{\frac{L\beta+j'}{2}}}{4\pi\Gamma(j')\Gamma(L\beta)(\Omega_i)^{\frac{L\beta+j'}{2}}} \times\left(\bar{\gamma}\right)^{-\frac{(L\beta+j')}{4}}E^{-M_1-\frac{L\beta}{4}-\frac{j'}{4}}\sum_{h=1}^{4}\prod_{m=1}^{4}\Gamma(b_m-b_h)^* \times\Gamma\left(1+b_h-(\frac{4-4M_1-L\beta-j'}{4})\right)\left((\frac{L\beta}{\Omega_i})^2\frac{1}{E2^4\bar{\gamma}}\right)^{b_h}. \quad (36)$$

The asymptotic BER of the system with EDFA at the Rx is given as $\tilde{P}_e = 1/2(\tilde{P}_e^{(1)}+\tilde{P}_e^{(2)})$ and it can be obtained from (35) and (36).

Further, let us discuss the diversity order of this system by observing the possible exponents of $\bar{\gamma}$ in (35) and (36). In asymptotic BER, only the terms corresponding to the smallest exponent of $\bar{\gamma}$ dominates. However, the discussion following (33) also applies to the asymptotic BER components (35) and (36). Therefore, all the terms corresponding to the indices p,i,j' in (35) and (36) will contribute to the asymptotic BER. Note that, one of the four terms from the vector $a_h=\{b_h+(L\beta+j')/4\}\in\{\frac{j'}{2},\frac{j'+1}{2},\frac{L\beta}{2},\frac{L\beta+1}{2}\}$, will appear as the exponent of $\bar{\gamma}$ in each of the summation terms of (35) and (36), which is the same as that of the system without EDFA. Since j' is the index with maximum value of α_i, when $\alpha < \beta$, then inside the summation with index

TABLE 1. Examples of different correlation models corresponding to different correlation levels with their respective Green's matrix approximations 3-Tx aperture-based systems.

Correlation matrices		Green's matrix approximation	
$\boldsymbol{\Sigma}^3_{arbit1} =$	$\begin{bmatrix} 1 & 0.4 & 0.1 \\ 0.4 & 1 & 0.4 \\ 0.1 & 0.4 & 1 \end{bmatrix}$	$\mathbf{C}^3_{arbit1} =$	$\begin{bmatrix} 1 & 0.386 & 0.149 \\ 0.386 & 1 & 0.386 \\ 0.149 & 0.386 & 1 \end{bmatrix}$
$\boldsymbol{\Sigma}^3_{circ1} =$	$\begin{bmatrix} 1 & 0.7 & 0.5 \\ 0.7 & 1 & 0.7 \\ 0.5 & 0.7 & 1 \end{bmatrix}$	$\mathbf{C}^3_{circ1} =$	$\begin{bmatrix} 1 & 0.726 & 0.52 \\ 0.726 & 1 & 0.726 \\ 0.52 & 0.726 & 1 \end{bmatrix}$
$\boldsymbol{\Sigma}^3_{const1} =$	$\begin{bmatrix} 1 & 0.6 & 0.6 \\ 0.6 & 1 & 0.6 \\ 0.6 & 0.6 & 1 \end{bmatrix}$	$\mathbf{C}^3_{const1} =$	$\begin{bmatrix} 1 & 0.699 & 0.473 \\ 0.699 & 1 & 0.699 \\ 0.473 & 0.699 & 1 \end{bmatrix}$
$\boldsymbol{\Sigma}^3_{const2} =$	$\begin{bmatrix} 1 & 0.9 & 0.9 \\ 0.9 & 1 & 0.9 \\ 0.9 & 0.9 & 1 \end{bmatrix}$	$\mathbf{C}^3_{const2} =$	$\begin{bmatrix} 1 & 0.886 & 0.784 \\ 0.886 & 1 & 0.886 \\ 0.784 & 0.886 & 1 \end{bmatrix}$

h, the terms with a_1 and a_2 as indices of $\bar{\gamma}$ will dominate the asymptotic BER; otherwise only the term corresponding to $\bar{\gamma}$ with index a_3 will contribute to the asymptotic BER. The aforementioned discussion leads to the diversity order of $G_d = L \min\{\frac{\alpha_1}{2}, \frac{\beta}{2}\}$ for the FSO-MIMO system with EDFA.

C. LOSS IN CODING GAIN DUE TO CORRELATION

The loss in coding gain ΔG_c^L due to correlation can be determined by taking the logarithmic of the ratio of G_c at two non-zero value of $\Sigma_{i,j} = \rho_1$ for $i \neq j$ and $\Sigma_{i,j} = \rho_2$ with $\rho_1 > \rho_2$ as follows:

$$\Delta G_c^L = 10 \log_{10} \left(\frac{G_c^{(\rho_1)}}{G_c^{(\rho_2)}} \right), \tag{37}$$

where $\rho_1 > \rho_2$. Moreover, for $\rho_1 < \rho_2$, the above expression becomes coding gain ΔG_c. Note that, G_c for a certain ρ can be calculated by comparing the derived asymptotic BER equation, $\tilde{P}_e$, with (32) and then substituting it in (37) to obtain ΔG_c^L. This parameter can also be obtained easily from the BER versus SNR plots by calculating the difference between the SNR levels required between two plots (at different correlation levels) to reach the same value of BER. Among the two plots, the one requiring lower SNR to reach the BER is said to be providing the coding gain over the other.

V. NUMERICAL RESULTS AND DISCUSSION

In this section, we present a detailed discussion of the comparative study of BER performance of the arbitrarily correlated FSO-MIMO system with and without the ASE noise. In order to check the validity of the proposed analytical results of Section IV, Monte Carlo simulation is performed to generate arbitrarily correlated $\Gamma\Gamma$ RVs following the algorithm proposed in [33]. The analytical results for the considered system with EDFA are obtained for parameters $M_1 = 2$, $E = 4$ and $y_{\text{th}} = 0.5$. Note that, in this paper we utilize the same set of parameters for EDFA that were used and validated in [20], [25]. Further, the choice of the AT parameter α_i for non-identical links in the rest part of this section can be verified from the AT parameters of the reported results in [39].

Considering the fact that, the inverse of the correlation matrix Σ does not always follow the tridiagonal property, following the similar algorithm as given in [35], we will approximate matrix Σ with another matrix $\mathbf{C}$ (Green's matrix approximation) such that $\mathbf{C}^{-1}$ is tridiagonal; and square of difference between the elements of matrices Σ and $\mathbf{C}$ is minimal. For Green's matrix approximation, it is required that $\mathbf{C}$ must be of the following form:

$$\mathbf{C} = \begin{bmatrix} x_1y_1 & x_1y_2 & \cdot & \cdot & x_1y_L \\ x_1y_2 & x_2y_2 & \cdot & \cdot & x_2y_L \\ \cdot & \cdot & \cdot & \cdot & \cdot \\ x_1y_L & x_2y_L & \cdot & \cdot & x_Ly_L \end{bmatrix}, \tag{38}$$

where x_i and y_i are two sequences of real numbers with $x_iy_i = 1$. Both the matrices Σ and $\mathbf{C}$ are equated to obtain a set of non-linear system equations. These equations can be easily solved using the widely known non-linear methods such as Levenberg-Marquardt, quasi-Newton or Conjugate gradient method, which are available in MATLAB, MATHEMATICA, etc. The validity and correctness of Green's matrix approximation method are studied in detail in [16] and [35]. By following the similar procedure outlined in [35], we have provided the numerical examples of three correlation models, i.e., linearly arbitrary, circular and constant, with their respective Green's matrix approximations, in Table 1, which will be used to obtain the analytical plots.

Figure 2 compares the simulated and analytical BER plots for the FSO-MISO system with two identical links for strong AT (i.e., $C_n^2 = 5 \times 10^{-13}$ m$^{-2/3}$), $\sigma_R^2 = 3.68$, $\alpha = 2$, $\beta = 1.4$, $L_1 = 0.95$ km and $\lambda = 1550$ nm [17]. RC is used as a spatial diversity technique in the proposed system and the results are obtained for both cases of with and without the ASE noise. The BER versus SNR plots are obtained for a constant correlation level of $\rho = 0.5$ and 0.95. A good agreement between the analytical and simulation results can be observed from the figure for both the correlation levels and the considered SNR range. It confirms the validity of the proposed analysis and also substantiates the correctness of the approximate approach followed for the analysis. First, let us discuss the results corresponding to the case with no ASE noise. A relative shift of the BER versus SNR plots along

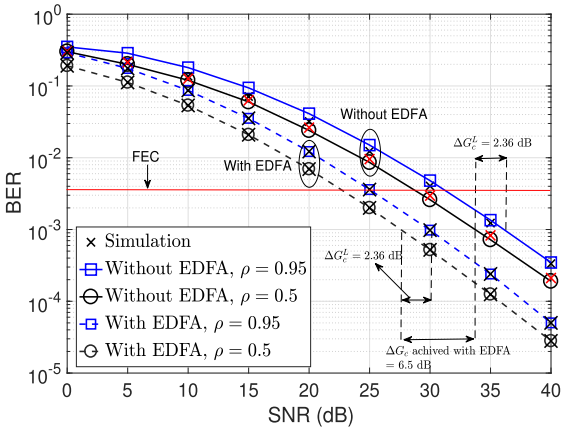

FIGURE 2. Comparison of analytical and simulated BER versus the average SNR for the 2-Tx lasers-based FSO-MISO system with and without pre-amplifier at Rx for strong AT with $\alpha = 2$, $\beta = 1.4$, $L_1 = 1$ km, $\lambda = 1550$ nm with various values of ρ.

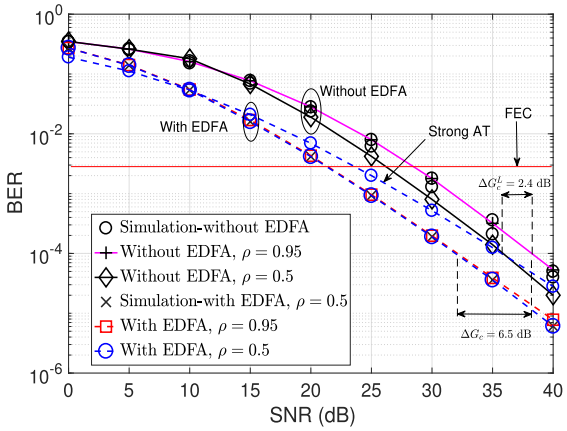

FIGURE 3. Comparison of analytical and simulated BER versus the average SNR for the 2-Tx lasers-based FSO-MISO system with and without pre-amplifier at the Rx for moderate AT with $\alpha = 4$, $\beta = 1.9$, $L_1 = 3$ km, $D = 15$ mm and $l_0 = 0$ with various values of ρ.

x-axis can be observed in Fig. 2, which signifies the performance degradation of the considered systems (i.e., in terms of ΔG_c^L) at high correlation levels among the system's apertures. Note that, there is a loss in the coding gain of 2.36 dB at a high correlation ρ of 0.95 as compared to $\rho = 0.5$ at a BER of 10^{-3} (which is just below the forward error correction (FEC) BER limit). However, as expected, with EDFA (pre-amplifier) at the Rx there is a significant coding gain of 6.5 dB compared with the case with no pre-amplifier.

Remark 1: For the considered values of AT parameters of $\alpha = 2$, $\beta = 1.4$, the diversity order G_d for the 2-Tx apertures-based system is β. Examples of the diversity order of the system are enumerated from Fig. 2, by taking the logarithm of the ratio of two BER values at the SNR values at a step of 10 dB for different values of ρ. For the system with no EDFA, we obtain the BERs of 2.1×10^{-4} and 2.9×10^{-3} at the SNR values of 40 dB and 30 dB, respectively for $\rho = 0.5$ from Fig. 1, which leads to a diversity order of 1.2 (i.e., close to β). By following the same process, G_d of the system with no EDFA at $\rho = 0.95$ is also obtained to be 1.2, which can approach β at very high SNR values. *It shows that, G_d is independent of ρ.* Similar sets of calculation are also repeated for the system with EDFA and the BERs of 2.8×10^{-5} and 5.2×10^{-4} are obtained at the SNR values of 40 dB and 30 dB, respectively for $\rho = 0.5$. This corresponds to the diversity order G_d of 1.3 and it remains unchanged with ρ at the considered SNR levels. *It shows that, G_d remains unaltered with the use of EDFA at the Rx.*[4]

In Fig. 3, we illustrate simulated and analytical BER versus SNR plots for the FSO-MISO system with two identical links under moderate AT, i.e., $\alpha = 4$ and $\beta = 1.9$ [1]. The values of α and β are obtained using (3) and (4), respectively for $L_1 = 3$ km, $\lambda = 1550$ nm, $C_n^2 = 1.7 \times 10^{-14}$ m$^{-2/3}$ and $\sigma_R^2 = 2.55$. It can be observed that, there is a good match between the simulated and analytical plots for the considered values of ρ and SNR. A SNR penalty of 2.2 dB at $\rho = 0.95$ compared with $\rho = 0.5$ at a BER of 10^{-4} is evident from the figure, for both the systems-with and without pre-amplifier. Moreover, at $\rho = 0.95$ the system with pre-amplifier offers an improved performance (i.e., a coding gain of 6.5 dB) compared to the system with no pre-amplifier. Further, in case of the system with pre-amplifier and for SNR values of <35 dB, both plots corresponding to ρ of 0.5 and 0.95 almost overlap. Nevertheless, for SNR > 35 dB both plots diverge and there is a loss in the coding gain at a high correlation level of 0.95. In this figure, BER plots corresponding to the strong AT at ρ of 0.5 is also shown for comparison with moderate AT at the same ρ. It can be observed that, there is an improvement in the BER performance in terms of the diversity order and the coding gain for the system under moderate AT (black dashed-circle marker) compared to the system under strong AT (red dashed-circle marker).

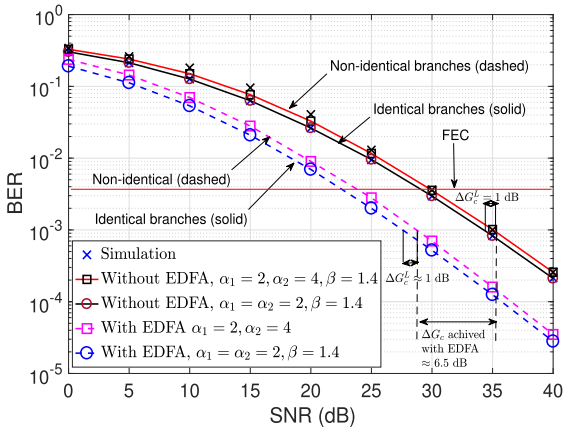

FIGURE 4. Comparison of BER performance of 2-Tx lasers-based system with identical links ($\alpha_1 = \alpha_2 = 2$, $\beta = 1.4$) and non-identical links ($\alpha_1 = 2$, $\alpha_2 = 4$, $\beta = 1.4$) in both the cases of with and without EDFA at $\rho = 0.5$.

Figure 4 illustrates a comparison of BER performance of the FSO-MISO system with $M = 2$ and $\rho = 0.5$ for

[4]This observation will be further validated by studying the diversity order of the considered system using asymptotic results.

two different cases of identical and non-identical links with and without EDFA at the Rx [20]. At first, both links are assumed to be identically distributed with $\alpha_1 = \alpha_2 = 2$ and $\beta = 1.4$. Then, without the loss of generality, it is assumed that large-scale AT parameters are in increasing order with $\alpha_1 = 2, \alpha_2 = 4$ and $\beta = 1.4$ [39]. Note that, the parameters corresponding to the non identical links, which resulted in $\alpha_1 = 2, \alpha_2 = 4$ and $\beta = 1.4$ are (i) for the link 1 with $L_1 = 950$ m, $C_n^2 = 5 \times 10^{-13}\text{m}^{-2/3}$, $\sigma_R^2 = 3.68$ and $\lambda = 1550$ nm, which results in $\alpha_1 = 2$ and $\beta = 1.4$.; and (ii) for the link 2 with $L_1 = 1200$ m, $C_n^2 = 12 \times 10^{-14}\text{m}^{-2/3}$, $\sigma_R^2 = 3.3$ and $\lambda = 1550$ nm, which results in $\alpha_2 = 4$ and $\beta = 1.4$. Although, the slopes in both cases remain unchanged, however, the system with identical links offers a marginal improvement in the coding gain by $\sim$1 dB compared to the system with non-identical links.

Observation 1: Note that, the offered coding gain at lower value of ρ (over higher values of ρ) is not dependent on EDFA. Moreover, the performance gain achieved for a 2×1 system with EDFA in case of the system with non-identical links remains the same as that of the system with identical links, i.e., $\approx$6.5 dB.

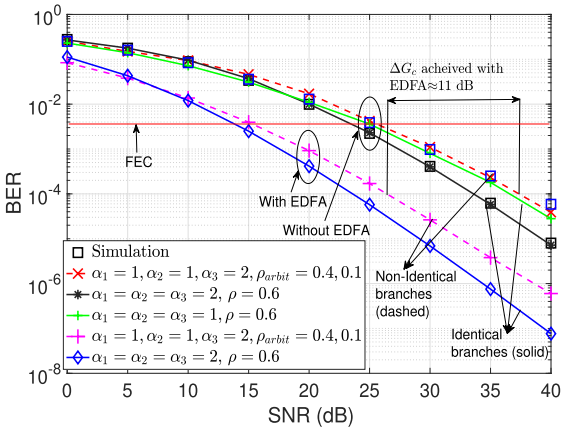

FIGURE 5. Analytical and simulation BER results of FSO-MISO system with $M = 3$ for identical and non-identical links at different correlation levels.

Figure 5 presents a comparison of analytical and simulated BER results for the 3×1 correlated FSO system with and without EDFA for (i) identically distributed links with $\rho = 0.6$; and (ii) non-identically distributed links with linearly arbitrary correlations, i.e., $\rho_{arbit} = 0.4, 0.1$, where ρ_{arbit} denotes the non-diagonal elements of the first row of the correlation matrix Σ. The plots are obtained for the arbitrary correlation matrix Σ^3_{arbit1} and the constant correlation matrix Σ^3_{const1}, as given in Table 1. For the system without EDFA at the Rx, it can be observed that the plot corresponding to the identical links with $\alpha_1 = \alpha_2 = \alpha_3 = 2, \beta = 1.4$ and $\rho = 0.6$ offer improved BER performance compared with the non-identical links with $\alpha_1 = \alpha_2 = 1, \alpha_3 = 2, \beta = 1.4$ and $\rho_{arbit} = 0.4, 0.1$. E.g., at a BER of 10^{-4}, the required SNRs are 33.5 and 37.5 dB for the identical and non-identical cases, respectively. Also shown is the BER result for the identical links for $\alpha_1 = \alpha_2 = \alpha_3 = 1$ and $\rho = 0.6$, which lies between the other two plots. With EDFA, we also observe similar trends for the identical case, which performs better than the non-identical scenario. Note that, the link with EDFA at the Rx offers a substantial coding gain of $\approx$ 11 dB, which means that to achieve a BER of 10^{-4} the link without EDFA will incur a high SNR penalty of 11 dB compared with the system with EDFA.

Remark 2: For the non-identically distributed links without EDFA (where $\min(\alpha_1, \beta) = \alpha_1$), the obtained BER values are 2.8×10^{-5} and 8×10^{-4} at SNRs of 40 and 30 dB, respectively for the correlation matrix Σ^3_{arbit1}. This corresponds to a diversity order of $1.45 \approx \frac{3\alpha_1}{2}$ with $\alpha_1 = 1$, see Fig. 5. In the case of the non-identical system with EDFA, the diversity order remains the same, i.e., $G_d \approx 1.5$. Now, let us consider the case of identical links system with EDFA, where the diversity order should be $G_d = \frac{3}{2}\beta = 2.1$ (from (33)). In this case, the obtained BER values are 7.6×10^{-8} and 6.9×10^{-6} at SNRs of 40 and 30 dB, respectively thus resulting in $G_d = 1.955 \approx \frac{3}{2}\beta$. It can be deduced from the results that, the diversity order is independent of the correlation model.

Contrary to the previously considered set-up where only a single aperture was considered at the Rx, in Fig. 6 the BER plots are shown for a 2×2 correlated MIMO system with and without EDFA and for four different non-identical links for $\alpha_1 = \alpha_2 = \alpha_3 = 1, \alpha_4 = 2$ and $\beta = 1.4$. In both cases, we obtain plots for the same scaling factor, i.e., $\Omega_i = 1$, $i = 1, 2, 3, 4$ and then for not necessarily the same scaling factor, i.e., $\Omega_i = 0.75$, $i = 1, 2, 3$ and $\Omega_4 = 1$. It is assumed that, the Tx apertures have a low level of correlation as compared with the Rx apertures with the following correlation matrices:

$$\Sigma^2_{Tx} = \begin{bmatrix} 1 & 0.15 \\ 0.15 & 1 \end{bmatrix}, \quad \Sigma^2_{Rx} = \begin{bmatrix} 1 & 0.3 \\ 0.3 & 1 \end{bmatrix}. \quad (39)$$

The effective correlation among all the sub-channels can be defined using Kronecker model of correlation as follows:

$$\Sigma^4_H = \Sigma^2_{Tx} \otimes \Sigma^2_{Rx} = \begin{bmatrix} 1 & 0.3 & 0.15 & 0.045 \\ 0.3 & 1 & 0.045 & 0.15 \\ 0.15 & 0.045 & 1 & 0.3 \\ 0.045 & 0.15 & 0.3 & 1 \end{bmatrix}, \quad (40)$$

where $\otimes$ denotes Kronecker product.

A good agreement between the analytical and simulation results is evident from Fig. 6, which validates the accuracy of the analysis carried out for the considered correlated FSO-MIMO system. At a BER of 10^{-4} for the system without EDFA, there is a SNR penalty is 2 dB at $\rho = 0.5$, as compared with $\rho = 0$. Moreover, it can be seen from the figure that, when all the links are assumed to have same scaling factor (as opposed to different scaling factor), it offers ΔG_c of $\approx$ 3 and 4 dB for the systems with and without EDFA, respectively. Note, ΔG_c of 12.5 dB offered by the system with EDFA compared with the system without EDFA. In order to calculate the diversity order of the considered FSO-MIMO

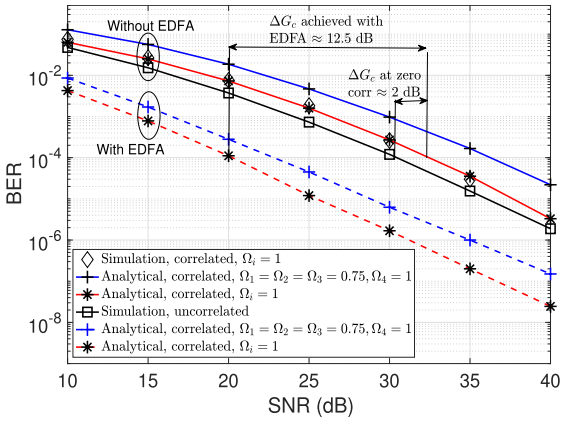

FIGURE 6. **Analytical and simulation BER results of 2 × 2 MIMO system with non-identical links at different correlation levels with $\alpha_1 = \alpha_2 = \alpha_3 = 1, \alpha_4 = 2, \beta = 1.4$.**

system, (33) is used, which gives $G_d = \frac{L}{2}\min\{\alpha_i, \beta\} = \frac{4}{2} \times 1 = 2$; this can be shown from Fig. 6. In case of the correlated MIMO system with EDFA, the BER values are 2.45×10^{-8} and 1.68×10^{-6} for SNRs of 40 and 30 dB, respectively. These values result in the diversity order G_d of $1.85 \approx 2$. Following the same approach for uncorrelated and correlated systems without EDFA we have $G_d \approx 2$.

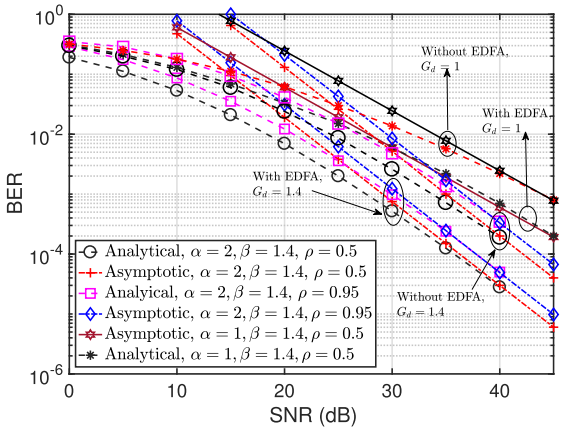

FIGURE 7. **Comparison of analytical and asymptotic BER plots for the 2-Tx lasers-based system corresponding to different levels of correlation illustrating the values of G_d under different AT regimes with and without EDFA at the Rx.**

Figure 7 illustrates comparison of the analytical and asymptotic BER results for a 2×1 system in order to verify the correctness of the proposed asymptotic analysis in Section IV. The results are obtained for two sets of AT parameters of $\alpha = 2, \beta = 1.4$ and $\alpha = 1, \beta = 1.4$ for $\rho = 0.5$ and 0.95. A very good match between the analytical and asymptotic results for SNR > 35 dB is observed from Fig. 7. Let us consider the FSO-MISO system with EDFA at $\rho = 0.95$ where the BER values are 6.02×10^{-6} and 0.00015 for SNRs of 45 and 35 dB, respectively. This gives $G_d = 1.4 = L/2 \times \beta$. Note that, the slopes of all plots corresponding to the same AT parameters (with and without EDFA) at any value of ρ are the same, see Fig. 7, which was not clearly evident in Fig. 2. Whereas, for the system with $\alpha = 1, \beta = 1.4$ we have G_d of 1.

TABLE 2. **Value of G_c obtained by comparing different parameters such as correlation (low and high), EDFA and no EDFA, Identical and non-identical links.**

L	ΔG_c (dB) (at low ρ)	ΔG_c(dB) (with EDFA)	ΔG_c (dB) (Identical links)
$L = 2$	2.36 - 2.2	6.5	1
$L = 3$	1- 0.8	11	4
$L = 4$	0.6-0.4	12.5	6

Table 2 summarizes the predicted results for ΔG_c for different set of parameters under different scenarios. We have compared the coding gain for $\rho = 0.5$ compared with $\rho = 0.95$ for $L = 2, 3, 4$. Note that, $L = 2, 3, 4$ corresponds to $M = 2, N = 1$, $M = 3, N = 1$, and $M = 2, N = 2$, respectively. It can be observed from the table that, the offered gain at low correlation keeps on reducing with increasing L. In other words, the SNR penalties at higher values of ρ reduces significantly with increasing L. The second column of Table 2 illustrates a substantial improvement in G_c offered by the system with EDFA (over the system without EDFA) at fixed values of ρ with L. For example, a correlated MIMO system with $L = 4$ offers an additional gain of 6 dB compared with the system with $L = 2$. Note that, employing EDFA at the Rx in a basic spatial diversity system with $L = 2$, results in a substantial coding gain of 6.5 dB. Finally, the coding gains of 1 and 4 dB are offered by the FSO-MISO system with $L = 2$ and 3 identical links (i.e., all $\alpha_i = 2$), respectively over the system with non-identical links (i.e., $\alpha_1 = \alpha_2 = \alpha_3 = 1$ and $\alpha_4 = 2$). Nevertheless, the SNR penalty incurred with the non-identical links depends on the values of AT parameters and it increases with growing L. Let us make the following observations about the numerical results.

Observation 2: It can be seen from Figs. 6 and 7 that, the slope of plots remains unchanged irrespective of any change in correlation level/model for a fixed number of Tx and Rx apertures. However, the diversity order improves with increasing number of Tx and/or Rx apertures. It can be deduced that, the diversity order of the proposed system is independent of the correlation matrix Σ, while it depends only on α, β and $L = M \cdot N$. It is in agreement with the derived expression of diversity gain (33).

Observation 3: Figs. 2-7 depict that, the diversity order remains unchanged even with EDFA at the Rx. However, with EDFA, a substantial coding gain is achieved compared to the system with no EDFA. Note, this gain increases with the number of Tx and/or Rx apertures.

Observation 4: It can be seen from Figs. 4-5 that, there is an SNR penalty in the system with non-identical links (not the same values of α in all links) as compared to the system with identical links. Note that, in Fig. 4 the plot corresponding to the identical links at comparatively higher ρ displays an improved performance than the one with non-identical

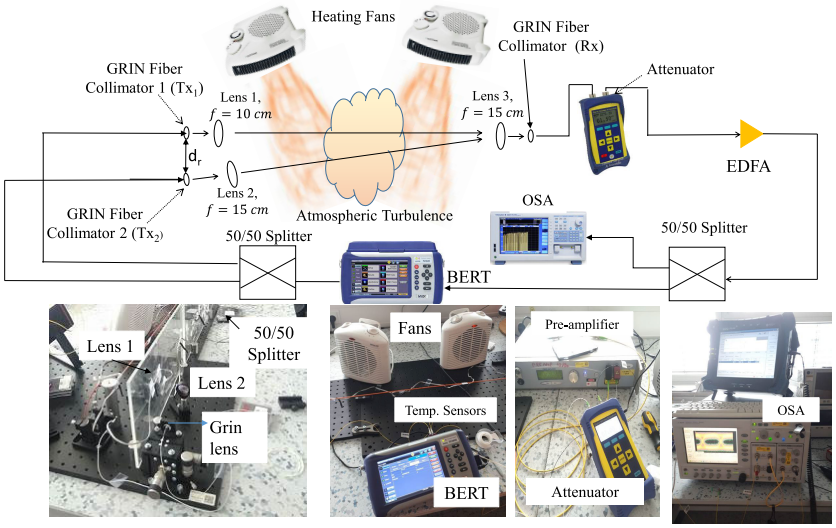

FIGURE 8. Experimental set-up of the correlated FSO-MISO system with EDFA.

links and a change in G_d. This is because of the change in $\min\{\alpha_1, \beta\}$ for both cases.

Observation 5: Figure 6 illustrates that, there is a loss in the coding gain incurred in the system with unbalanced links, i.e., Ω_i not necessarily the same for all links, as compared to the system with balanced links. Note that, the system with balanced links will offer coding gains over the system with unbalanced links only when $\Omega_i^{(\text{balanced})} \geq \max\{\Omega_i^{(\text{unbalanced})}\}$.

VI. EXPERIMENTAL INVESTIGATION

In the previous section, we established with the analytical results that, a coding gain is offered by - the system with low ρ over the system with high ρ, the system with EDFA over the system without EDFA, the system with identical/balanced links over the system with non-identical/unbalanced links. Note that, it is difficult to measure BER practically over the FSO wireless links without using EDFA. Therefore, in this section, we outline the experimental set-up developed [5] for a FSO system over a turbulent channel with EDFA at the Rx and measure the BER for different values of ρ.

1) EXPERIMENTAL SET-UP

The laboratory experimental set-up for the correlated FSO system shown in Fig. 8 is composed of two Tx apertures (i.e., Tx_1, Tx_2), a FSO channel with a link length L_1 of 3 m, and a Rx. In RC, the same symbol sequence is transmitted simultaneously by both Txs. We have used a signal source (BER tester - BERT-VeEX VEPAL TX300) to generate a pseudo-random binary data pattern in the NRZ-OOK format at a data rate of 10 Gb/s and wavelength 1550 nm. The generated data sequence is launched into a single mode fiber (SMF) and then applied to 50/50 beam splitter (Thorlabs OSW22-1310E). The light signals from both Txs (i.e., SMFs) are launched into the free space channel using a combination of gradient-index (GRIN) fiber optic collimators (Thorlabs 50-1550A-APC) and plano-convex lenses (aperture of 2.54 cm) with focal lengths of 10 and 15 cm, respectively. At the Rx side, a plano-convex lens with f of 15 cm and a GRIN fiber collimator are used to couple the incoming optical beam into SMF. The output of SMF is attenuated using a digital variable attenuator in order to adjust the level of optical SNR (OSNR), prior to being amplified using a EDFA. The output of the EDFA is applied to 50/50 beam splitter for monitoring the received signal quality using an optical spectrum analyzer (OSA) and a BERT. The BER is measured using the correlated set-up for different turbulence levels and correlation values using the BERT. As for the free space channel, we have used a controlled indoor AT channel to create turbulence by blowing hot air using two fans perpendicular to the direction of the propagating optical beams. The strength of turbulence is controlled by adjusting the speed/heating level of the fans. We have used 20 temperature sensors spaced 0.225 m apart along the link in order to record the temperature profile along the propagation path. The measured temperatures are used to determine C_n^2 using the equation given in [46]. Note that, for the FSO channel to be uncorrelated the Tx apertures must be separated by the spatial coherence distance exceeding the fading correlation length [1]. In addition, the correlation level depends on various factors such as the angle of arrival, L_1, σ_R^2, C_n^2 and λ (see Eq. (8)). Since the components used in the experiment are not of the microscopic size in practical outdoor FSO links, it is practically infeasible to attain the aperture separation of the order of λ. Therefore, we have placed the apertures as close as possible to ensure a correlated channel and evaluated ρ using (8).

2) EXPERIMENTAL RESULTS

We have recorded the measured data for the FSO link span of 3 m for two different cases. Case A - Both heating fans were

[5]The experimental set-up was developed at Czech Technical University in Prague.

on and placed near the transmitting end. Note, the channels were completely separated near Txs using barriers (as shown in Fig. 8) to maintain $\rho \approx 0$. In order to obtain different values of ρ, the measurements were recorded at $d_r = 13.5$, 10 and 6.5 cm, where d_r denotes the distance between the Txs. Note, (i) the barriers were removed to achieve highly correlated channels; and (ii) the speed and heating level of fans were used to generate different AT levels. Case B - Only placed the fans at receiving end and repeated the same procedure as in Case A.

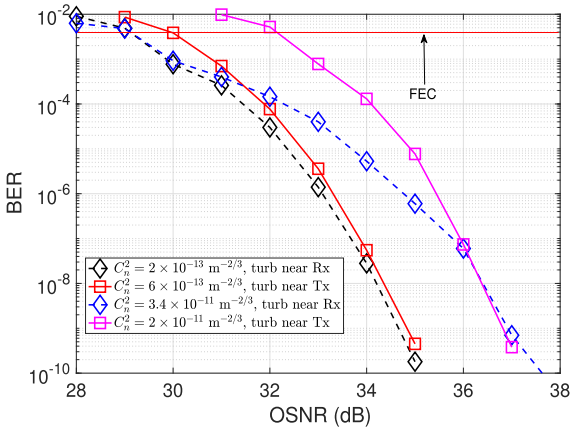

FIGURE 9. Experimental BER versus OSNR results of a 2 × 1 FSO-MISO system at different turbulence levels and $d_r = 10$ cm illustrating the comparative study of impact of turbulence at the Tx and at the Rx.

Figure 9 shows the measured BER as a function of the optical SNR for a range of AT levels generated at the Tx and Rx ends. First, we measured the BER for $d_r = 10$ cm, with C_n^2 of $\sim 10^{-13}$ m$^{-2/3}$ and $\rho = 0.7$, which corresponds to moderate-strong AT. Note that, ρ is determined using (8), see Section II-C. It can be seen from the figure that, at lower OSNR values of < 31 dB, the BER performance is slightly better when fans are placed near the receiving end compared to the fans being positioned at the transmitting end. However, for OSNR > 31 dB, the measured BER values are almost similar for both cases. Further, keeping other parameters the same we placed the barrier between the Txs and we measured the strong turbulence regime (i.e., C_n^2 of $\sim 10^{-11}$ m$^{-2/3}$) and $\rho \approx 0$. It can be observed from Fig. 9 that, in order to maintain a BER of 10^{-4} under strong AT, the required OSNRs are 32 and 34 dB when fans were placed near the receiving and transmitting ends, respectively. It means that, the coding gain is reduced by 2 dB when the turbulence source was near the Txs. This is because the optical wave-front experiencing both phase and amplitude distortions, thus leading to a much weaker and dispersed signal at the receiving end.

Finally, Fig. 10 shows the measured BER versus the OSNR for a 2×1 correlated FSO-MISO link for a range of AT levels, when fans were placed near the transmitting end. Note, for $d_r = 13.5$ cm, the calculated average value of turbulence is $C_n^2 = 1.7 \times 10^{-14}$ m$^{-2/3}$ and $\rho = 0.9$. The BER is recorded for this set-up and the measurement is repeated by reducing

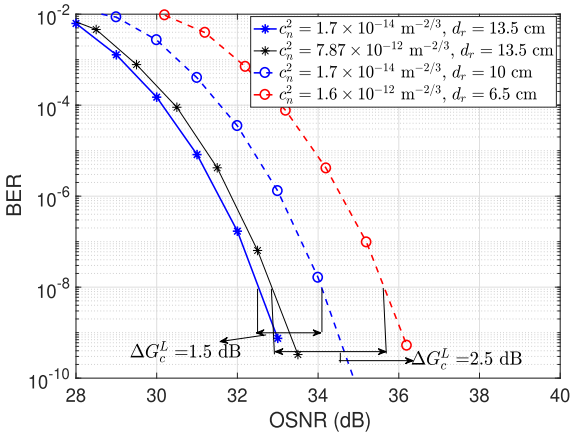

FIGURE 10. Experimental BER versus OSNR results of a 2 × 1 correlated FSO-MISO system at different turbulence levels and different values of ρ illustrating ΔG_c achieved at lower values of ρ.

d_r to 10 cm and maintaining C_n^2 to be the same as in the previous case. For this separation of Txs the calculated value of ρ is 0.97. Note that, there is a loss in coding gain ΔG_c^L of 1.5 dB at $d_r = 10$ cm compared to d_r of 13.5 cm. Next, we increased the AT levels to $C_n^2 = 1.6 \times 10^{-12}$ m$^{-2/3}$ and 7.9×10^{-12} m$^{-2/3}$ for $d_r = 6.5$ cm ($\rho \approx 0.3$) and 13.5 cm ($\rho = 0$), respectively and recorded the BER. In the case of strong AT with $C_n^2 = 1.6 \times 10^{-12}$ m$^{-2/3}$, a loss in the coding gain ΔG_c^L of 2.5 dB is observed from the figure because of higher correlation level ρ of 0.3.

Remark 3: At a certain C_n^2 value, a relative shift of BER plots along x-axis is evident from Fig. 10 with increasing correlation level (decreasing d_r), which denotes the loss in coding gain at higher correlation level as compared with a lower correlation level. This experimental observation is in agreement with the analytical results of 2 × 1 FSO system shown in Fig. 2 (also summarized in row 2 - column 2 of Table 2), which shows a loss in the coding gain of 2.2-2.36 dB at higher ρ as compared with the lower ρ.

VII. CONCLUSION

We investigated analytically and experimentally, the impact of correlation and the ASE noise on the BER performance of the FSO-MIMO system employing RC. A novel and a simple BER analytical expressions for the proposed correlated FSO-MIMO system with and without EDFA at Rx was derived. In order to validate the analytical results, simulated BER results were obtained, and a close match between the analytical and simulation results was observed for the considered SNR range. Asymptotic behaviour of the considered system was thoroughly analysed with the help of derived closed-form expressions of the asymptotic BER, diversity order, coding gain and loss in the coding gain of the system. With the help of proposed analysis, it was shown analytically that, any variation in the correlation level and employing EDFA at the Rx did not affect the diversity order of the system. Nevertheless, a 2 × 1 system with EDFA at the Rx offered a substantial coding gain of 6.5 dB (at a BER

of 10^{-3}) over similar system without EDFA, and this gain was shown to be increasing with the number of Tx/Rx apertures. Moreover, significant degradation in the BER performance was observed at a higher correlation of $\rho = 0.95$ in terms of the loss in coding gain of 2.2 dB, which was validated through experiments. Further it was observed that, the considered system with identically distributed turbulence along links offered improved performance compared with the system with non-identical links.

REFERENCES

[1] Z. Ghassemlooy, W. Popoola, and S. Rajbhandari, *Optical Wireless Communications: System and Channel Modelling With MATLAB*. Boca Raton, FL, USA: CRC Press, 2012.

[2] M. Uysal, C. Capsoni, Z. Ghassemlooy, A. Boucouvalas, and E. Udvary, *Optical Wireless Communications—An Emerging Technology*. Cham, Switzerland: Springer, 2016.

[3] M. A. Khalighi and M. Uysal, "Survey on free space optical communication: A communication theory perspective," *IEEE Commun. Surveys Tuts.*, vol. 16, no. 4, pp. 2231–2258, 4th Quart., 2014.

[4] G. T. Djordjevic, M. I. Petkovic, J. A. Anastasov, P. N. Ivanis, and Z. M. Marjanovic, "On the effects of correlation on outage performance of FSO-unbalanced multibranch SC receiver," *IEEE Photon. Technol. Lett.*, vol. 28, no. 12, pp. 1348–1351, Jun. 15, 2016.

[5] X. Zhu and J. M. Kahn, "Maximum-likelihood spatial-diversity reception on correlated turbulent free-space optical channels," in *Proc. IEEE Conf. Global Telecommun.*, vol. 2, Dec. 2000, pp. 1237–1241.

[6] M. R. Bhatnagar and Z. Ghassemlooy, "Performance analysis of gamma–gamma fading FSO MIMO links with pointing errors," *J. Lightw. Technol.*, vol. 34, no. 9, pp. 2158–2169, May 1, 2016.

[7] A. Jaiswal, M. R. Bhatnagar, and V. K. Jain, "Performance evaluation of space shift keying in free-space optical communication," *J. Opt. Commun. Netw.*, vol. 9, no. 2, p. 149, Feb. 2017.

[8] Y.-Y. Zhang, H.-Y. Yu, J.-K. Zhang, Y.-J. Zhu, J.-L. Wang, and T. Wang, "Full large-scale diversity space codes for MIMO optical wireless communications," in *Proc. IEEE Int. Symp. Inf. Theory*, Jun. 2015, pp. 1671–1675.

[9] E. Bayaki and R. Schober, "On space-time coding for free-space optical systems," *IEEE Trans. Commun.*, vol. 58, no. 1, pp. 58–62, Jan. 2010.

[10] M. Safari and M. Uysal, "Do we really need OSTBCs for free-space optical communication with direct detection?" *IEEE Trans. Wireless Commun.*, vol. 7, no. 11, pp. 4445–4448, Nov. 2008.

[11] X. Song and J. Cheng, "Subcarrier intensity modulated MIMO optical communications in atmospheric turbulence," *J. Opt. Commun. Netw.*, vol. 5, no. 9, p. 1001, Sep. 2013.

[12] M. Abaza, R. Mesleh, A. Mansour, and E.-H.-M. Aggoune, "Spatial diversity for FSO communication systems over atmospheric turbulence channels," in *Proc. IEEE Wireless Commun. Netw. Conf. (WCNC)*, Apr. 2014, pp. 382–387.

[13] K. Peppas, G. Alexandropoulos, C. Datsikas, and F. Lazarakis, "Multivariate gamma-gamma distribution with exponential correlation and its applications in radio frequency and optical wireless communications," *IET Microw. Antennas Propag.*, vol. 5, no. 3, p. 364, Feb. 2011.

[14] N. D. Chatzidiamantis and G. K. Karagiannidis, "On the distribution of the sum of gamma–gamma variates and applications in RF and optical wireless communications," *IEEE Trans. Commun.*, vol. 59, no. 5, pp. 1298–1308, May 2011.

[15] G. Yang, M. A. Khalighi, Z. Ghassemlooy, and S. Bourennane, "Performance evaluation of correlated-fading space-diversity FSO links," in *Proc. IWOW*, Oct. 2013, pp. 71–73.

[16] J. Zhang, M. Matthaiou, G. K. Karagiannidis, and L. Dai, "On the multivariate gamma-gamma distribution with arbitrary correlation and applications in wireless communications," *IEEE Trans. Veh. Technol.*, vol. 65, no. 5, pp. 3834–3840, May 2016.

[17] R. Priyadarshani, M. R. Bhatnagar, Z. Ghassemlooy, and S. Zvanovec, "Effect of correlation on BER performance of the FSO-MISO system with repetition coding over gamma–gamma turbulence," *IEEE Photon. J.*, vol. 9, no. 5, pp. 1–15, Oct. 2017.

[18] T. Ismail, E. Leitgeb, Z. Ghassemlooy, and M. Al-Nahhal, "Performance improvement of FSO system using multi-pulse pulse position modulation and SIMO under atmospheric turbulence conditions and with pointing errors," *IET Netw.*, vol. 7, no. 4, pp. 165–172, Jul. 2018.

[19] M. Al-Nahhal and T. Ismail, "Enhancing spectral efficiency of FSO system using adaptive SIM/M-PSK and SIMO in the presence of atmospheric turbulence and pointing errors," *Int. J. Commun. Syst.*, vol. 32, no. 9, pp. 1–13, Jun. 2019.

[20] P. A. Humblet and M. Azizoglu, "On the bit error rate of lightwave systems with optical amplifiers," *J. Lightw. Technol.*, vol. 9, no. 11, pp. 1576–1582, Nov. 1991.

[21] D. Marcuse, "Derivation of analytical expressions for the bit-error probability in lightwave systems with optical amplifiers," *J. Lightw. Technol.*, vol. 8, no. 12, pp. 1816–1823, Dec. 1990.

[22] A. O. Aladeloba, A. J. Phillips, and M. S. Woolfson, "Improved bit error rate evaluation for optically pre-amplified free-space optical communication systems in turbulent atmosphere," *IET Optoelectron.*, vol. 6, no. 1, pp. 26–33, Jan. 2012.

[23] B. Chan and J. Conradi, "On the non-Gaussian noise erbium-doped fiber amplifiers," *J. Lightw. Technol.*, vol. 15, no. 4, pp. 680–687, Apr. 1997.

[24] A. Mathur, P. Saxena, and M. R. Bhatnagar, "Performance of optically pre-amplified FSO system under ASE noise with pointing errors," in *Proc. IEEE Annu. India Conf. (INDICON)*, Dec. 2016, pp. 1–6.

[25] P. Saxena, A. Mathur, and M. R. Bhatnagar, "BER performance of an optically pre-amplified FSO system under turbulence and pointing errors with ASE noise," *IEEE J. Opt. Commun. Netw.*, vol. 9, no. 6, pp. 498–510, Jun. 2017.

[26] P. Saxena, A. Mathur, and M. R. Bhatnagar, "Performance of optically pre-amplified FSO sytem under gamma-gamma turbulence with pointing errors and ASE noise," in *Proc. IEEE 85th Veh. Technol. Conf. (VTC Spring)*, Jun. 2017, pp. 1–5.

[27] P. Saxena, A. Mathur, and M. R. Bhatnagar, "BER of an optically pre-amplified FSO system under Málaga turbulence, pointing errors, and ASE noise," in *Proc. IEEE 28th Annu. Int. Symp. Pers., Indoor, Mobile Radio Commun. (PIMRC)*, Oct. 2017, pp. 1–6.

[28] B. Wu, B. Marchant, and M. Kavehrad, "Dispersion analysis of 1.55 μm free-space optical communications through a heavy fog medium," in *Proc. IEEE Global Telecommun. Conf.*, Nov. 2007, pp. 527–531.

[29] M. Bouhadda, F. M. Abbou, M. Serhani, F. Chaatit, and A. Boutoulout, "Analysis of dispersion effect on a NRZ-OOK terrestrial free-space optical transmission system," *J. Eur. Opt. Soc. Rapid Publ.*, vol. 12, no. 1, pp. 1–6, Oct. 2016.

[30] M. R. Bhatnagar, "A one bit feedback based beamforming scheme for FSO MISO system over gamma–gamma fading," *IEEE Trans. Commun.*, vol. 63, no. 4, pp. 1306–1318, Apr. 2015.

[31] O. M. Hasan, "Bit error rate and outage rate results for non-zero turbulence cells over gamma-gamma free-space optical wireless channel," *J. Opt. commun.*, vol. 34, pp. 385–391, Dec. 2013.

[32] G. Yang, M. A. Khalighi, Z. Ghassemlooy, and S. Bourennane, "Performance evaluation of receive-diversity free-space optical communications over correlated gamma-gamma fading channels," *Appl. Opt.*, vol. 52, no. 24, pp. 5903–5911, Aug. 2013.

[33] Z. Song, K. Zhang, and Y. L. Guan, "Generating correlated Nakagami fading signals with arbitrary correlation and fading parameters," in *Proc. IEEE Int. Conf. Commun. (ICC)*, vol. 3, Jun. 2002, pp. 1363–1367.

[34] J. M. Garrido-Balsells, A. Jurado-Navas, J. F. Paris, M. Castillo-Vázquez, and A. Puerta-Notario, "Spatially correlated gamma-gamma scintillation in atmospheric optical channels," *Opt. Express*, vol. 22, no. 18, pp. 21820–21833, Sep. 2014.

[35] G. Karagiannidis, D. Zogas, and S. Kotsopoulos, "An efficient approach to multivariate Nakagami-*m* distribution using green's matrix approximation," *IEEE Trans. Wireless Commun.*, vol. 2, no. 5, pp. 883–889, Sep. 2003.

[36] M. Mansour Abadi, Z. Ghassemlooy, S. Zvanovec, M. R. Bhatnagar, M.-A. Khalighi, and Y. Wu, "Impact of link parameters and channel correlation on the performance of FSO systems with the differential signaling technique," *J. Opt. Commun. Netw.*, vol. 9, no. 2, pp. 138–148, Feb. 2017.

[37] J. Reig, M. A. Martinez-Amoraga, and L. Rubio, "Generation of bivariate Nakagami-*m* fading envelopes with arbitrary not necessary identical fading parameters," *Wireless Commun. Mobile Comput.*, vol. 7, no. 4, pp. 531–537, May 2007.

[38] G. Arfken, *Mathematical Methods for Physicists*, 3rd ed. Orlando, FL, USA: Academic, 1985.

[39] G. Karagiannidis, N. Sagias, and T. Tsiftsis, "Closed-form statistics for the sum of squared Nakagami-*m* variates and its applications," *IEEE Trans. Commun.*, vol. 54, no. 8, pp. 1353–1359, Aug. 2006.

[40] M. Win, G. Chrisikos, and J. Winters, "MRC performance for M-ary modulation in arbitrarily correlated Nakagami fading channels," *IEEE Commun. Lett.*, vol. 4, no. 10, pp. 301–303, Oct. 2000.
[41] A. P. Prudnikov, Y. Brychkov, and O. I. Marichev, *Integrals and Series: More Special Functions*, vol. 3, G. G. Gould, Ed. Moscow, Russia: Nauka Publishers, 1990.
[42] Q. Cao, M. B. Pearce, and S. C. Wilson, "Free space optical MIMO system using PPM modulation and a single optical amplifier," in *Proc. 2nd Int. Conf. Commun. Netw. China*, Aug. 2007, pp. 1113–1117.
[43] I. S. Gradshteyn and I. M. Ryzhik, *Table of Integrals, Series, and Products*, 7th ed. New York, NY, USA: Academic, 2007.
[44] T. J. I. Bromwich, *Introduction to the Theory of Infinite Series*, 3rd ed. Chelsea, U.K.: AMS, 1991.
[45] M. R. Bhatnagar and Z. Ghassemlooy, "Performance evaluation of FSO MIMO links in gamma–gamma fading with pointing errors," in *Proc. IEEE Int. Conf. Commun. (ICC)*, Jun. 2015, pp. 5084–5090.
[46] L. C. Andrews, R. L. Phillips, and C. Y. Hopen, *Laser Beam Scintillation With Applications*, vol. PM99. Bellingham, WA, USA: SPIE, 2001.

RICHA PRIYADARSHANI (Student Member, IEEE) was born in India, in 1988. She received the B.Tech. degree in electronics engineering from Uttar Pradesh Technical University, India, in 2010, and the M.E. degree in wireless communications engineering from the Birla Institute of Technology, Mesra, Ranchi, India, in 2013. She is currently pursuing the Ph.D. degree from the Indian Institute of Technology Delhi, Delhi, India. She has held the position of an Assistant Professor at Amity University, India, for two and half years before joining the Ph.D. degree. Her research interests include free space optical communication, visible light communication, and MIMO systems.

MANAV R. BHATNAGAR (Senior Member, IEEE) received the M.Tech. degree in communications engineering from the Indian Institute of Technology Delhi (IIT Delhi), New Delhi, India, in 2005, and the Ph.D. degree in wireless communications from the Department of Informatics, University of Oslo, Oslo, Norway, in 2008.

From 2008 to 2009, he was a Postdoctoral Research Fellow with the University Graduate Center (UNIK), University of Oslo. He held visiting appointments at the Wireless Research Group, IIT Delhi, the Signal Processing in Networking and Communications (SPiNCOM) Group, University of Minnesota Twin Cities, Minneapolis, MN, USA, the Alcatel-Lucent Chair, SUPELEC, France, the Department of Electrical Computer Engineering, Indian Institute of Science, Bangalore, India, UNIK, University of Oslo, the Department of Communications and Networking, Aalto University, Espoo, Finland, and the INRIA/IRISA Laboratory, University of Rennes, Lannion, France. He is currently a Professor with the Department of Electrical Engineering, IIT Delhi, where he is also a Brigadier Bhopinder Singh Chair Professor. His research interests include signal processing for multiple-input-multiple-output systems, cooperative communications, non-coherent communication systems, distributed signal processing for cooperative networks, multiuser communications, ultrawideband-based communications, free-space optical communication, cognitive radio, software-defined radio, power line communications, molecular communications, and satellite communications.

Dr. Bhatnagar is a Fellow of the Institution of Engineering and Technology (IET), U.K., the Indian National Academy of Engineering (INAE), the National Academy of Sciences, India (NASI), the Institution of Electronics and Telecommunication Engineers (IETE), India, and the Optical Society of India (OSI). He has received the NASI-Scopus Young Scientist Award 2016 in engineering category, the Shri Om Prakash Bhasin Award in Electronics and Information Technology, in 2016, and the Hari Om Ashram Prerit Dr. Vikram Sarabhai Research Award 2017. He was selected as an Exemplary Reviewer of the IEEE Communications Letters, in 2010 and 2012, and the IEEE Transactions on Communications, in 2015. He was an Editor of the IEEE Transactions on Wireless Communications, from 2011 to 2014.

JAN BOHATA (Member, IEEE) was born in Prague, Czech Republic, in 1988. He received the B.S. and M.S. degrees in communications, electronics, and multimedia from the Faculty of Electrical Engineering, Czech Technical University in Prague, in 2012, and the Ph.D. degree in radio electronics, in 2018.

In 2012, he joined the Wireless and Fiber Optics Group, Department of Electromagnetic Field with a main focus on microwave photonics, fiber and free space optics networks, and optical communications in harsh environments. He is the author of more than 30 journal and conference papers and involved in a number of national and European research projects.

Dr. Bohata is a member of OSA.

STANISLAV ZVANOVEC received the M.Sc. and Ph.D. degrees from the Faculty of Electrical Engineering, Czech Technical University (CTU) in Prague, in 2002 and 2006, respectively. He is currently works as a Full Professor, the Deputy Head of the Department of Electromagnetic Field, and the Chairperson of Ph.D. Branch with CTU. His current research interests include free space optical and fiber optical systems, visible light communications, OLED, RF over optics, and electromagnetic wave propagation issues for millimeter wave band. He is the author of two books (and coauthor of the recent book *Visible Light Communications: Theory and Applications*), several book chapters and more than 250 journal articles and conference papers.

ZABIH GHASSEMLOOY (Senior Member, IEEE) received the C.Eng. degree, the B.Sc. degree (Hons.) in electrical and electronics engineering from Manchester Metropolitan University, U.K., in 1981, and the M.Sc. and Ph.D. degrees from the University of Manchester, U.K., in 1984 and 1987, respectively. From 1987 to 1988, he was a Postdoctoral Research Fellow with City University, U.K. From 2004 to 2014, he was the Associate Dean of research with the School of Engineering, and the Faculty of Engineering and Environment, Northumbria University, Newcastle. He was a Research Fellow, in 2016, and a Distinguished Professor, in 2015, with the Chinese Academy of Science, Quanzhou. He is currently the Head of the Optical Communications Research Group. He has published 825 articles (328 journals and eights books), 97 keynote/invited talks, and supervised 64 Ph.D. degree students. His research interests include optical wireless communications, free space optics, visible light communications, and radio over fibre/FSO. He is a Fellow of IET and a Senior Member of OSA. He was the IEEE UK/IR Communications Chapter Secretary, from 2004 to 2006, the Vice Chairman, from 2006 to 2008, the Chairman, from 2008 to 2011, and the Chairman of the IET Northumbria Network, from 2011 to 2015. He has been the Vice Chair of the OSA Technical Group of Optics in Digital Systems, since 2018, and the Chair of the IEEE Student Branch with Northumbria University, since 2019. He is also the Chief Editor of the *British Journal of Applied Science and Technology* and the *International Journal of Optics and Applications*, an Associate Editor of a number of international journals, and a Co-Guest Editor of a number of special issues.